,Christoph Kappler[1*], Knut Kaiser[1], Phillipp Tanski[2], Friederike Klos[3], Alexander Fülling[4], Almut Mrotzek[5], Michael Sommer[6], Oliver Bens[1]

Stratigraphy and age of colluvial deposits indicating Late Holocene soil erosion in northeastern Germany

[1]GFZ German Research Centre for Geosciences, Telegrafenberg, D-14473 Potsdam, Germany

[2]Freie Universität Berlin, Institute of Geographical Sciences, Malteser Straße 74-100, D-12249 Berlin

[3]Technical University Bergakademie Freiberg, Institute of Geology, Bernhard-von-Cotta-Straße 2, D-09599 Freiberg

[4]Humboldt University of Berlin, Institute of Geography, Unter den Linden 6, D-10099 Berlin, Germany

[5]University of Greifswald, Institute of Botany and Landscape Ecology, Soldmannstraße 15, D-17487 Greifswald

[6]Leibniz Center for Agricultural Landscape Research (ZALF) e.V., Institute of Soil Landscape Research, Eberswalder Strasse 84, D-15374 Müncheberg, Germany

*Corresponding author: Christoph.kappler@gmail.com

Keywords

- historic and prehistoric soil erosion
- geochronology
- palaeosol
- geoarchaeology
- landscape development

Abstract

In the focus of this study are the sedimentary characteristics, chronology, magnitude, and causes of past soil erosion dynamics of an agriculturally intensively used glacial lowland landscape. From the mesoscale Quillow river catchment, sedimentary sections bearing colluvial sediments from different landforms were analysed to explore their geoarchive potential and to establish a local chronology of Late Holocene soil erosion. Sections from footslopes contain a rather simple stratigraphy with one topping colluvial horizon of up to 1 m thickness burying a palaeosol. In contrast glacial kettle holes preserve more complex sequences partly having several colluvial layers with intercalating palaeosols. The most complex stratigraphy is associated with a kettle hole being the ultimate sediment trap for a dendritic gully system, forming a 4 m thick sequence of alternating peat and colluvial layers. Thirty OSL ages and 13 radiocarbon ages are used to reconstruct phases of soil erosion. Potentially human-induced soil erosion, which is corroborated by local archaeological and palynological data, can be traced back to the last c. 4000 years. The oldest colluvial deposits date back to the Late Bronze Age. Most datings, however, cluster within the last 600 years with a peak in the last 200 years, ascribing the main phase of local soil erosion to the recent past. Thus, although numerous archaeological finds are detected in the catchment since the Neolithic, considerable agricultural soil erosion does not occur before the last millennium. A compilation of OSL chronologies based on colluvial sediments from other regions in Central Europe shows a more complex erosion history there with a pronounced two- or three-phased distribution of ages primarily dating into the last c. 4000-5000 years. This study underlines that in northeastern Central Europe human impact on landscapes was effective apparently at a later stage as compared to some adjacent regions.

1 Introduction

Present-day landscapes are the result of various natural and anthropogenic processes. Many European landscapes have been intentionally modified by humans (e.g. by deforestation and agricultural activities) surely since the Neolithic and probably already since the Late Palaeolithic/Mesolithic period (e.g. Gramsch, 2000; Ryan & Blackford, 2010; Tolksdorf et al., 2013). The conversion of naturally vegetated areas into agricultural land, the intensification of soil management and land-use changes generally led to significantly increased soil erosion rates (Dotterweich, 2008; Vanwalleghem et al., 2017). In Central Europe, the onset of Neolithic economy introduced by the linear pottery culture people around 6 to 7 kiloyears (ka) BP (Bogucki, 1996; Gronenborn et al., 2014; Svizzero, 2015) potentially marks a drastic change in various landscape characteristics and processes, such as land cover, mesoclimate and solid matter fluxes. Beside human impact, changes in soil erosion rates are also linked to past climate changes and extreme meteorological events (e.g. the 1342 AD event in Central Europe; Dotterweich, 2013; Herget et al., 2015).

Research on prehistoric and historic soil erosion in central and western Europe have focused mainly on specific geomorphological settings and sub-thematic issues, namely on gully systems (e.g. Dotterweich et al., 2003; Schmitt et al., 2006; Dreibrodt et al., 2010a), on the input of sediments into valleys, rivers and lakes (e.g. Lang et al., 2003a; Dreibrodt and Bork, 2005; Hoffmann et al., 2013), and on the formation and distribution of colluvial sediments (e.g. Lang, 2003; Dreibrodt et al., 2010b; Fuchs et al., 2010). Further motivation to study human-induced soil erosion in the region came from geoarchaeological issues (e.g. Tinapp et al., 2008; Dreibrodt et al., 2013; Lubos et al., 2013).

Recent pedological research in the study area generally focusses on the nexus of water balance, soil erosion and matter fluxes in a strongly agriculturally used landscape (Wilken et al., 2017; Herbrich et al., 2017), implying, among others, the question how present-day soil erosion patterns are to be interpreted in a long-term, i.e. centennial to millennial perspective. Therefore, this study aims to analyse the sedimentological-pedological characteristics, chronology, magnitude, and causes of past soil erosion dynamics within a river catchment which is part of the global change TERENO observatories of the Helmholtz Association (Zacharias et al., 2011; Bogena et al., 2012; Pütz et al., 2016; www.tereno.net). Particularly, a sufficient number of geochronological datings is expected to allow insights into the history of colluvial sedimentation on a larger scale and to investigate if the colluvial dynamics are influenced by the landform on which they were deposited.

As a hypothesis, we assume a long lasting erosion pattern since this geomorphologically diverse area represents an old cultural landscape with a high number of prehistoric and historic archaeological sites (Fig. 1).

2 Study area

The catchment of the Quillow river covers an area of 168 km^2 and is located in the hummocky glacial landscape of the Weichselian glacial belt ('young morainic area') of northeastern Germany. The end moraine of the *Gerswalder Staffel* runs from the northwest to the southeast in the western part of the Quillow river catchment (Supplement 1). The elevation varies between 18 m a.s.l. in the east to 120 m a.s.l. in the west of the study area (Fig. 1). The surficial sediments were mainly deposited during the Pomeranian phase (W2) of the Weichselian glaciation around 20 ka ago according to recalculated cosmogenic ages from erratics (Hardt and Böse, 2016) and luminescence age data from glaciofluvial deposits (Lüthgens et al., 2011). The area was completely deglaciated around 15 to 14 ka (Lüthgens et al., 2011). The hilltops and slopes consist mainly of sand-covered till and intercalated layers of glaciofluvial sand, whereas the valleys are filled by fine-grained fluvial sand and peat and gyttja (Supplement 1). Locally, dendritic gully systems have incised in steep slopes (elevation between 67-115 m a.s.l.) with gully lengths of up to 120 m and depths of up to 8 m (Supplement 2E).). The soil pattern of the agricultural land is a result of prolonged erosion and deposition processes. Only 10-15 % of the area consists of soils unaffected by soil erosion (Luvisols, Stagnosols, Arenosols). Convex hilltops and steep slopes are dominated by extremely eroded A-C profiles (Calcaric Regosols, soil classification according to IUSS Working Group WRB, 2015). Luvisols showing different degrees of erosion cover the up- and midslopes. From the footslopes to the depressions a sequence of Gleyic-Colluvic Regosols, Mollic Gleysols and (buried) Terric Histosols has developed (Deumlich et al., 2010; Janetzko and Schmidt, 2014). In the eastern part of the catchment degraded Phaeozems and Chernozems occur. Their formation and preservation is interpreted to result from the specific natural and land use conditions of the Uckermark region, i.e. high carbonate contents in the parent material, high clay content and subcontinental climate with relatively low annual precipitation, and specifics of the land-use history since the Neolithic (Fischer-Zujkov et al., 1999).

The Quillow river catchment belongs to the upper Ucker river catchment draining to the Baltic Sea (Fig. 1). The river originates in Lake Parmener See in the western catchment and drains after a 27 km flow length with discharge rates between 0.3 and 2.8 m^3s^{-1} at Prenzlau into the Ucker river.

The Quillow river catchment can be regarded as an assemblage of drainless (sub-) catchments, first connected by artificial ditches probably built since the 13^{th} century AD draining to the Ucker river (Enders, 1992). A patchwork of small drainless depressions, called (glacial) kettle holes, occurs. Within the Quillow river catchment there are more than 5000 of these small depressions, often having a diameter of a few decametres only. 1300 of which are filled with water, whereas the rest is filled with mineral soil and peat (Kalettka and Rudat, 2006; Lischeid et al., 2017; Nitzsche et al., 2017). They originated mostly from melting of buried stagnant ice, usually called ‘dead ice’ (e.g. Kaiser et al., 2012). After the melting of these ice ‘plombs’, water-filled basins of varying size could appear, which were later often replaced by mires and, if small enough, completely covered by colluvial sediments (Borówka 1992; Karasiewicz et al., 2014).

The climate of the Quillow river catchment is characterised by an east-west gradient from 450 to 600 mm mean annual precipitation and a mean annual air temperature ranging from 8.5 to 7.5 °C (Nitzsche et al., 2017). The present-day land cover of the Quillow river catchment consists of arable land and pasture (70 %), wetlands and lakes (16 %), forest (11 %) and settlements (3 %; Schneider, 2014).

3 Material and methods

3.1 Field research

In 2014, several landforms, representing partly intermittent sedimentary sinks such as footslopes, kettle holes, floodplains and alluvial fans, were identified and explored with hand-drillings (n = 631) using an universal gouge auger with 1 m segments and coring depths of up to 4 m. Eleven reference soil pits were dug, one mire depression was cored with percussion drilling and one trench at the footslope of a kettle hole was excavated. The soil pits were dug to a depth of 2 m or less, ensuring that the complete Holocene sedimentary sequence was recorded. The walls of the profiles were cleaned, documented by photographs and the soil horizons were recorded and sampled according to the guidelines of the German soil classification standard (Ad-hoc AG Boden, 2005). Soil colours were described according to the

MUNSELL colour scheme, and each horizon was sampled for grain size and soil organic carbon (SOC) analyses. Some horizons of each profile were sampled for radiocarbon dating and optically stimulated luminescence dating (OSL).

3.2 Soil and sediment classification

Soils were classified according to the German soil classification standard Ad-hoc AG Boden (2005). Additionally, soil types were classified according to the IUSS Working Group WRB standard (2015). However, the designation of colluvial horizons bears a potential for misunderstandings, depending on the national scientific convention. For instance, the English ‘colluvium’, comprising Pleistocene and Holocene deposits, is less strictly defined than the German term ‘Kolluvium’ (Kleber, 2006), which in its most rigid form is defined as a Holocene deposit created on slopes by flowing water due to man-induced soil erosion (Ad-hoc AG, 2005; Leopold and Völkel, 2007).

In general, colluvial sediments represent poorly sorted deposits whose transport and sedimentation took place gravitationally by water or tillage erosion. Material was often transported over short distances (e.g. Van Vliet-Lanoë, 1998; Bertran and Texier, 1999). Some definitions of the term colluvium include all slope deposits, whereas others restrict its occurrence to footslopes excluding fluvial processes or including the latter (cf. Miller and Juilleret, 2016). In the with respect on colluvial sediments rather sophisticated Polish classification system the term ‘colluvium’ is used for slope sediments created by mass movements, while the term ‘deluvium’ describes deposits originating from slope wash and the term ‘proluvia’ is used for sediments connected to gully erosion. Further, sediments originating from anthropogenic denudation, as induced by agricultural activities, are called ‘tillage diamictons’ (Twardy, 2011; Kittel, 2014). Although Ad-hoc AG Boden (2005) defines ‘M’ as a Holocene soil sediment, in this study all soil horizons, despite knowing the age, are described/classified as M if they exhibit features of transported solum. Additionally, both Pleistocene and Holocene mostly poorly sorted and mostly sandy sediments on slopes and valley floors with more or less organic content, are named ‘colluvial’.

3.3 Laboratory analyses

3.3.1 Sediment analysis

Sediment samples (n = 108) were sieved to 2 mm, coarser material (> 2 mm) was weighed and the percentage of the total weight was calculated. Sediment < 2 mm was treated with H_2O_2 to remove any soil organic matter (SOM) and dispersed with dissolved tetra-sodium pyrophosphate ($Na_4P_2O_7 * 10H_2O$) applied for 24 hours in an overhead shaker. The samples were then analysed in a laser particle size analyser using laser diffraction spectroscopy (HORIBA LA-950). The organic carbon content was determined using an Elemental Analyser (Euro EA3000, EuroVector). Samples with a volume of 1 cm^3 were freeze-dried, milled and prepared as 5 mg aliquots in Sn capsules. Additional 3 mg aliquots were decalcified in Ag capsules with 20 % HCl and dried at 85 °C to measure total organic carbon (TOC).

3.3.2 Geochronological analyses

Prior to OSL dating luminescence measurements were carried out on densely taken (distance c. 10 cm) sediment samples (n = 224) with a portable SUERC OSL reader in order to screen the suitability of the profiles for OSL dating (Sanderson and Murphy, 2010). This approach saves resources since unbleached samples could be discarded before they enter the sample preparation and measurement process. The samples for OSL dating (n = 31) were taken horizontally from the walls of the profiles using steel tubes with a diameter of 50 mm from a freshly cleaned position, where light exposed material had instantly been removed before. In the laboratory, sample material from only the inner parts of the filled steel tubes was prepared using standard procedures of the OSL lab of Humboldt University (Berlin). The sediment samples were first sieved to separate the grain size fraction of 90 to 200 µm. After removal of carbonates and organic matter with HCl (10 and 30 %) and H_2O_2 (10 and 30 %), quartz grains were extracted applying density separation with heteropolytungstate heavy liquid (LST, 2.75 and 2.62 g/cm^3). The subsequent etching with hydrofluoric acid (40 %, 60 min) eliminated any potential feldspar contamination and removed the alpha irradiated outer layer of the grains (~ 20 µm). Small multiple grain aliquots with a diameter of 2 mm, containing c. 200 grains, were prepared (Duller, 2008). The OSL samples were measured on a Risø TL-DA 15 reader using the standard single-aliquot regenerative (SAR) protocol (Murray and Wintle, 2000) . A preheat test was carried out on sample HUB-562 to define appropriate preheat settings. Dose recovery tests were then conducted on all samples to test whether a known laboratory dose can be recovered properly using a SAR protocol with the previously determined preheat procedure. Sets of 24 or 48 aliquots per sample were stimulated with blue LED light ($\lambda = 470 \pm 30$ nm) at 125 °C for 40 s. The resulting OSL signals were detected through a Hoya U340 filter ($\lambda = 330 \pm 40$ nm). The preheat temperature was set to 200 °C (10 s), the test dose cut-heat temperature to 160 °C. High resolution gamma ray spectrometry was applied to estimate the sediment dose rates arising from the decay of primordial radionuclides (HPGe detector). The cosmic ray dose rates were estimated based on geographical position, elevation and burial depths (Prescott and Hutton, 1988, 1994). The Central Age Model (CAM) and the Minimum Age Model (MAM) were applied to calculate the equivalent doses (Galbraith et al., 1999). The equivalent dose distributions were statistically analysed to decide between the two age models. Dose distributions showing overdispersions exceeding 20 % in combination with a significant positive skew were analysed with the MAM, otherwise the CAM was applied. Large equivalent dose scatters were supposed to indicate insufficient daylight exposition during transport typical for this sediment type. (Galbraith et al., 1999; Galbraith and Roberts, 2012). Luminescence ages in this study are reported as years (a) or kiloyears (ka), since the term ‘BP’ is reserved to radiocarbon ages according to Brauer et al. (2014).

Radiocarbon dating (n = 13) was carried out on organic material embedded in sediments, where luminescence dating does not allow for reliable burial ages or where additional chronological control of the profile was needed. In the sediment core NM-6 (from a mire at Naugarten (Figs. 1-3, Supplement 2E) plant macro-remains (wood, needles, sphagnum moss) from intercalated peat layers were dated. Furthermore, from two adjacent profiles charred plant material and charcoal were used to date buried soils. The radiocarbon measurements were carried out in the Poznań Radiocarbon Laboratory using accelerated mass spectrometry (AMS). Calibration was performed with the program OxCal v4.2.3 (Bronk Ramsey, 2009a) using the IntCal13 atmospheric calibration curve (Reimer et al., 2013). Radiocarbon ages are reported as years or kiloyears cal BP showing the 2-sigma confidence range.

3.4 Age data and statistics

For the obtained luminescence ages, Kernel Density Estimates (KDE) were computed using a self-developed algorithm in the statistical programming environment R. From the luminescence age and its standard error an age range was calculated and ‘filled’ with 10^6 artificial uniformly distributed ages. Subsequently, the kernel density was calculated for each simulated age within the respective error range using the R function ‘density()’. This approach is necessary since the true age is not normally but uniformly distributed within the standard deviation of luminescence ages (Galbraith, 2010; Vermeesch, 2012). For a better understanding the cumulative distribution of ages was plotted onto the KDE plot.

4 Results

4.1 General material characteristics

The colluvial horizons analysed (n = 28) originate from different sedimentary environments, yet their textural composition is mainly limited to sand, loamy sand and sandy loam with a share of clay mostly below 10 % and silt below 50 %. Only few horizons consist of loam and silt loam (Fig. 4A).

The TOC-content of the colluvial horizons ranges with the median of 0.6 % between 0.4 and 1.1 % (Fig. 4B).

The reference (key) profiles are presented in the following according to their geomorphological context (depositional environment) differentiated into the categories foot slopes, kettle holes, gully systems and valley floors.

4.2 Foot slopes

The profiles were situated at the lower part of slopes and exhibited at first glance a uniform stratigraphy (profiles FKHG2, CHRIST1, TSU9, TSU17, RAAK2; Supplement 2). All these profiles are located in intensively agriculturally used areas. The main stratigraphical feature is a colluvial layer of on average more than 1 m thickness consisting of weakly sorted loamy to silty sand with SOC-contents between 0.1 and 1.2 % (Tab. 1) derived from the hilltops. In profiles CHRIST1 and RAAK2 two pedological units with a buried soil below one or two colluvial layers respectively could be recorded (Figs. 1, 2, 3). The deposition of the colluvial sands above the palaeosols started around 162 ± 20 a and 615 ± 97 a, respectively. Both datings represent minimum age estimates due to incomplete bleaching. In both profiles, a Phaeozem developed on Pleistocene loamy till, was buried by colluvial sand, yielding in RAAK2 a mean age of soil development (cf. Alexandrovskiy & Chichagova, 1998) of 3828-3640 a cal BP. At site Lake Tiefer See (Fig. 1, Supplement 2I), two profiles were analysed close to the shoreline of a small lake. In both profiles, buried soils are covered by a homogenous more than 1 m thick Colluvic Regosol consisting of silty sand. At TSU09 a burial age of 330 ± 30 a was obtained, whereas in TSU17 the palaeosol got buried around 810 ± 60 a. Two further datings from the middle of the colluvial layer yield (minimum) ages of 120 ± 20 a (TSU09) and 190 ± 20 a (TSU17). In FKHG2 (Figs. 1, 2, 3) two Colluvic Regosols have developed from colluvial sand on the lower slope adjacent to the Quillow river. The intercalated colluvial layer (II M) yielded an age of 2466 ± 194 a. A second palaeosol (II fAh) has developed in that layer and was buried around 680 ± 55 a.

The obtained OSL ages of slope deposits represent the onset of erosion phases terminating a stability phase which is indicated by the palaeosols. The detected (pre-) historic erosion dynamics have occurred on slopes in the Quillow river catchment since the last 2400 a with a distinct increase in the last 800 a (Fig. 5B). Within the latter period two peaks can be observed around 200 and 650 a ago.

4.3 Kettle holes

When surrounded by arable land, kettle holes represent a potentially perfect sink for eroded deposits, recording the erosion history of very local catchments. Four profiles from the margin of three kettle holes were analysed (STF2, STF3, FKHG1, CHRIST647). As a common feature, these profiles show a more differentiated stratigraphy of colluvial deposits and intercalated palaeosols than the profiles located on slopes.

The kettle hole Steinfurth (STF) has a slightly convex slope with a length of approximately 150 to 200 m and a height difference from the watershed to the centre of the depression of about 10 m (Supplement 2). The kettle hole itself measures 260 m from north to south. At the margin of the eastern footslope a 41 m long trench was excavated (Fig. 1, Supplement 2F). Colluvial layers and intercalated palaeosols were recorded (Fig. 6) and two key profiles (STF2, STF3) were studied in detail. The lower profile STF3 consists of five sedimentological units. The loamy till at the base of the profile at 3.2 m depth with a Late Pleistocene age of 14.6 ± 1.2 ka is followed by c. 40 cm of black humic sand with a SOC content of 1.8 % dated to 6195 ± 520

a. A layer of lacustrine sand with 90 cm thickness deposited around 3693 ± 233 a is overlain by 30 cm of strongly decomposed peat. A massive colluvial layer of sandy loam with 1.3 m thickness completes the profile. The onset of sedimentation of the colluvium was dated to 526 ± 77 a.

The upslope profile STF2 exhibits a colluvial wedge, which interrupted the formation of a palaeosol (Fig. 6). The profile consists of loamy till at its base, followed by a layer of lacustrine sand with an age of 10.8 ± 0.7 ka. This old age results presumably from unbleached sand. Above, a strongly humic soil horizon was found which is divided by a wedge of colluvial sand dated to 3135 ± 205 a (II M). The formation of the younger strongly humic soil horizon took place after the deposition of the colluvial wedge halted and finally got buried by the uppermost colluvium around 1124 ± 71 a.

It is apparent that on the slope of the Steinfurth kettle hole, slope wash occurred in the Late Bronze Age, interrupting the formation of the Ah horizon which continued to form afterwards. Furthermore, the succession of terrestrial, semi-terrestrial and sub-aquatic sediment types provides evidence on the palaeohydrology of the depression. The lacustrine sands deposited during the Atlantic period indicate a higher water level in the kettle hole.

The kettle hole with the profile CHRIST647 at its margin has a straight slope with a length of 60 m from the watershed to the centre of the depression with a height difference of 8 m and a diameter of 48 m (Supplement 2D). The profile bears at its bottom in 1.9 m depth a buried Gleysol with a mean radiocarbon age of 6883-6676 a cal BP, followed by a colluvial layer (IV M) of 10 cm thickness (Figs. 2, 3). Above that layer, a strongly mineralised buried Histosol of 25 cm thickness (III fHa) yielding a radiocarbon age of 3167-2960 a cal BP was found. Another colluvial layer of c. 25 cm thickness merges into a second buried Gleysol (II fGor-Ah) with a radiocarbon age of 436-152 a cal BP. This Gleysol is buried by the uppermost colluvial layer of 1.1 m thickness.

The kettle hole profile FKHG1 is located at the margin of the depression and bears two buried soils with a colluvial layer on top (Figs. 2, 3). The profile reaches 2 m whereas the lower 40 cm consist of lacustrine sand and the upper 1.6 m consist of colluvial brownish silty sand. The two buried Mollic Gleysols (III fAa, II fAa) have developed in lacustrine sand. However, we cannot exclude the possibility that these buried soils represent redeposited humic sands. They are separated by a 30 cm thick layer of greyish lacustrine sand (II ilC) dated to 377 ± 38 a. The onset of colluvial sedimentation dates to around 216 ± 27 a.

According to the kettle holes sections, slope erosion occurred during different periods of time, the first ranging from approx. 3.95 to 2.9 ka, the second dates to 1.1 ka, and the third peak covers the last approx. 500 a (Fig. 5C).

4.4 Gully systems

Two profiles from the gully system at Naugarten were studied enabling a complex local erosion history (Fig. 1). Correlative colluvial sediments were transported over short distances only (c. 75 m in maximum) filling up several small depressions which form a sediment trap cascade. The final sediment trap of this system is a kettle hole (c. 100 m in diameter) called ‘Naugartener Moor’ (mire). Core NM6 was drilled in this mire down to a depth of 4 m, yielding a sequence of five peat layers and five colluvial sand layers (Figs. 2, 3; Supplement 2E).

According to the measurements with the portable OSL-reader, most of the quartz grains in the OSL samples from NM-6 did not experience any bleaching during the erosion and transportation process. Only for the uppermost and lowermost OSL samples, reasonable results were obtained. Thus, the age model for the core is based on radiocarbon datings of plant remains from the intercalated peat layers. The 400 cm long core bears greyish glaciofluvial sand at its base deposited at 15.6 ± 1.3 ka. The overlying 370 cm exhibit five peat layers of 10 to 70 cm thickness with five intercalated layers of coarse colluvial sand, in parts with a gravel content of up to 25 %. The peat layers date from 3210-2885 to 1291-1181 a cal BP. One radiocarbon dating yielded an age of 254-32 a cal BP which does not fit in the age sequence and is, therefore, excluded as unreliable. The profile is topped with a 50 cm thick layer of colluvial coarse sand dating to 280 ± 40 a.

Uphill from this depression two profiles (NAU11, NAU13) were investigated in the direct vicinity of the gully outlets (Supplement 2E). Profile NAU11 is located at the eastern margin of a local basin and exhibits a buried soil developed in glaciofluvial sand dated to around 12.6 ± 1.5 ka ago (Fig. 2). The fossil Ah horizon at the profile base was buried by colluvial (in parts layered) sediments at 760 ± 100 a. In this colluvial material a secondary Cambi-/Luvisol has developed, indicated by a deeply developed fossil B horizon (IV fB(t)v), showing erosional features at its top. The upper 80 cm of the profile consist of banded sand layers containing illuviated clay bands. The lowermost colluvium (III M) yielded a minimum deposition age of 1190 ± 21 a. This reflects an age inversion, probably due to insufficient bleaching.

Profile NAU13, located only 40 m upslope from core NM6 (Supplement 2E), shows a buried charcoal kiln (cf. Raab et al., 2015) at its base (Fig. 2). The kiln is indicated in the profile by charcoal pieces of up to 10 cm diameter within a buried black II fojAh horizon and the lateral enrichment of charcoal around the profile within a diameter of 3.5 m. A charcoal sample from this layer gave an age of 736-669 a cal BP. The kiln was built onto a fossil Cambisol developed in re-deposited glaciofluvial sand with an age of 2090 ± 360 a. Colluvial sand consisting of several distinct horizons (IV M, III M, II M, M) buried the kiln at 640 ± 70 a and continued to aggrade at least until 280 ± 20 a ago. The central colluvial layer (III M) appears to be weathered more strongly due to its distinct brownish colour and iron coating on sand grains. It might represent eroded soil material of a former Cambisol, originally located upslope of the profile, or developed in-situ after sedimentation.

Further evidence of local colluvial sedimentation connected with gullying was detected next to the shore of Lake Großer See (Fig. 1). Here an alluvial fan (length 145 m; width 108 m) aggraded distantly to several gullies. The gullies are up to 95 m long and up to 10 m deeply incised in the undulating relief to the west of the lake (Supplement 2A). Profile GRAUHG1 is located in the central part of the alluvial fan. It is divided into several layers consisting of colluvial sand and two buried soils developed in them . The radiocarbon age of 294-73 a cal BP from the lowermost gleyic horizon (V elGro) is assumed to be too young as it shows an age inversion in the age sequence with the youngest age at the bottom of the profile (Fig. 2). As the dating was carried out on wood the deviation might be caused by modern root material. This layer consists of silty sand in which a Mollic Gleysol (V fAh) developed. This soil was buried by colluvial sand (IV M) at 422 ± 61 a ago. A second soil developed in this layer, however, to a lesser intensity than the underlying palaeosol. The upper edge of this IV fAh horizon shows sharp erosion features to the following colluvial sand layer (III M), dated to 242 ± 21 a. The upper half of the profile consists of brownish sand with a slightly developed Ah horizon at its top.

According to the luminescence datings, the incision of the analysed gullies occurred in the last 2000 a with a majority of luminescence ages placed in the last 800 a (Fig 5). Special attention has to be paid to the radiocarbon dated core NM-6, since it represents a particularly well-differentiated profile containing five colluvial layers with intercalated dated peat layers. These layers indicate alternating phases of gully incision and landscape stability since the last 3200 a until the very recent past.

4.5 Valley floors

Valley floors represent a further geoarchive type in the Quillow river catchment which also records soil erosion. Numerous auger corings revealed similar stratigraphic sequences, consisting of till at the base, followed by (glacio-) fluvial sands in which a former Fluvisol has developed, buried by colluvium (with thicknesses between 0.3 and more than 1 m).

Profile RAAK1 (Fig. 1) is located within the valley floor of the Quillow river (Supplement 2B). It consists of 70 cm of (glacio-?) fluvial sand at its base dated to 13.7 ± 1.06 a ago, in which a Fluvisol has developed. The radiocarbon age of charcoal extracted from the buried soil (II fAh) yielded an unreliable age of 520-330 a cal BP, most likely due to the very low content of carbon (0.14 mg C) or translocation of the sampled organic matter by biota. The transition from the palaeosol into the overlying colluvium is diffuse, indicated by a transitional horizon (M-fAh), overlain by 50 cm of colluvial silty sand. The deposition of the colluvium was dated to a minimum age of 1133 ± 136 a.

According to the data a locally abandoned channel of the Quillow river was buried by colluvial sand during the Early Middle Ages. It must be taken into account that only 15 % of the land surface in the Quillow river catchment is directly linked to the river by surface runoff due to the high percentage of small closed watersheds (i.e. kettle holes; Nitzsche et al., 2017). The rather old age of the (glacio-) fluvial sand at the base suggests that this river section exists since the late Pleistocene.

5 Discussion

5.1 Late Holocene soil erosion in the upper Ucker river catchment

Prior to the discussion of the local results, some general aspects on triggers of soil erosion and the potential of their detection shall be reflected. Tillage and (concentrated) surface runoff are considered as the dominant triggers of local soil erosion (e.g. Sommer et al., 2008; Wilken et al., 2017), whereas further processes, such as randomly occurring natural features including tree fall, animal tracks or wildfire, may also contribute to the erosion and translocation of topsoil. However, the unambiguous attribution of the specific process responsible for soil erosion remains in most cases unclear or cannot be confirmed unequivocally. In an old cultural landscape such as the Quillow river catchment surely different anthropogenic as well as natural processes led to the detected development of the soil profiles. A connection of colluvial layers to former land use activities can be proven rather unambiguously if settlements are located in the close vicinity of the studied profiles (e.g. Szwarczewski, 2009; Lubos et al., 2011; Kittel, 2014; Kittel, 2015; Küster et al., 2015). Direct indicators for past land-use are plough marks found in colluvial layers (Schatz, 2000; Twardy, 2011) or charcoal kilns which indicate adjacent deforestation (Larsen et al., 2013).

The stratigraphies suggest, that soil erosion occurred in the Quillow river catchment mainly in the last 4000 a. There was only one exception, i.e. the colluvial layer IV M in kettle hole CHRIST647, which dates between c. 3000 and c. 6600 a. The KDE plot (Fig. 5A) shows six maxima in the onset of deposition, hence erosion at 300 a, 700 a, 1100 a, 2400 a, 3400 a and 3600 a. Figures 5B-D suggest, that the erosional dynamics depend to a certain extent on the type of the landform investigated. The slope processes occurred mainly in the last 800 a and only in one case at around 2400 a, whereas kettle holes are more likely to also preserve older slope deposits.

As shown by colluvial layers, which are thinner than 20 cm and embedded between buried soils (STF2, STF 3, CHRIST647), kettle holes are even able to record short-term erosional phases, because they are closed depressions and, thus, form the ultimate sediment trap in the local sediment cascade. Similar observations were reported from other sites in northeastern Germany, where the most differentiated stratigraphies were recorded at the margins of kettle holes (e.g. Kaiser et al., 2000; Küster et al., 2011).

The colluvial wedge intercalated in the fAh-horizon in profile STF2 yielded a deposition age of 3135 ± 205 a, thus dating into the Late Bronze Age. Since the wedge neither buries the whole palaeosol nor the slope, an erosional process with only local impact seems plausible. Water erosion or an extreme precipitation event probably would have eroded much more material and transported or deposited this over the entire slope. Human forcing, as a potential cause for erosion, could be supported by the close location of a Bronze Age settlement 200 m upslope (Supplement 2, F). In the Randow river valley, c. 30 km to the east, Schatz (2000) found several superimposed signatures of ploughing in a layer of prehistoric colluvium which may be assigned to the same time period with first arable activities. Furthermore, from that period onwards, human-induced higher erosion rates and first significant formation of slope deposits were reported throughout Central Europe (Szwarczewski, 2009; Klimek, 2010; Zádorová et al., 2013; Vogt, 2014; Kittel, 2015).

At the slopes of the agriculturally intensively used Quillow river catchment, most of the former stratigraphic record has probably got lost, due to strong tillage activity since historic times (Sommer et al., 2008; Kleeberg et al., 2016). The only evidence of prehistoric slope processes was found in profile FKHG2, where a colluvial sand layer dated to 2466 ± 192 a. This layer can potentially be ascribed to past farming activities, supported by the non-stratified (potentially ploughed) habitus of the II M horizon and by the adjacent location of an Iron Age settlement (Supplement 2, G). The well-developed overlying palaeosol (II fAh) indicates a subsequent phase of landscape stability. However, the onset of colluviation in most profiles was dated to the last 600 to 200 a, mainly due to the large-scale conversion of forested areas into arable land in the Quillow river catchment (Schneider, 2014; Wulf et al., 2016). For the western part of the catchment an increase from 45 % amount of arable land in 1780 AD to 72 % in 2000 AD was suggested (Wulf et al., 2016). Five dates of colluvial layers point to the High to Late Middle Ages (RAAK2, NAU13, FKHG2, NAU11, TSU17), forming a dating interval from 1145 to 1497 AD. For Central Europe, this is a well-known period with high erosion rates and very intensive formation of colluvia (e.g. Zolitschka et al., 2003; Dotterweich, 2008; Dreibrodt et al., 2010b; Twardy, 2011).

Thus, most of the profiles analysed in this study represent a modern land-use history, mainly of the last 500 to 700 a. In some profiles (e.g. TSU9) the relation of age and thickness of the colluvium indicates an extraordinary increase in deposition, hence erosions rates, during the last century (Frielinghaus and Vahrson, 1998; Sommer et al., 2008).

The formation of the gully systems at Naugarten and Grauenhagen (Fig. 1) seems to be linked to land-use changes, supported by the colluvial burial of a charcoal kiln in profile NAU13 at 640 ± 70 a and the deposition of an alluvial fan at GRAUHG1 whose sedimentation started at 422 ± 61 a. At Naugarten, the map by Schmettau (1767) already depicts the gullies incised into the slope. At that time, the forest boundary was recorded beyond its current position. Based on the age of the buried charcoal kiln, deforestation is assumed to have been responsible for the erosive dynamics detected between the 13th to 15th centuries AD. At Grauenhagen, Sobietzky (2008) identified four glassworks which were in operation during the 18th century AD. In close vicinity to the gully system a glasswork operated from 1735 to 1765 AD. Thus, a relationship between the land-cover change due to the glasswork industry, causing local deforestation, and gully formation seems appropriate.

The depression 'Naugartener Moor' (NM6) represents the ultimate sediment trap for the gully system located in the surroundings, indicating alternating phases of input of colluvial sand and peat formation during the last c. 3000 a. The Bv horizons in the lower parts of the profiles NAU11 and NAU13 suggest a relatively long-lasting landscape stability prior to their burial. Profile NAU13, located c. 15 m upslope of section NM-6, allows an attribution to human-induced erosion for the last c. 700 a only.

The uppermost OSL date from NAU11 can be considered as too old due to incomplete bleaching indicated by the bimodal De-Distribution (HUB-615, Suppl. 3). The middle OSL date in NAU11 yielded with 760 ±100 a (1155-1355 AD) and a unimodal distribution a reasonable result (HUB-613, Suppl. 3). Hence the burial of the former surface at NAU11 is dated to the same period in which the kiln was buried at site NAU13. Deforestation for charcoal production could, therefore, be considered as a potential trigger for gully erosion in this phase. As the construction of the kiln indicates a stable surface as late as 1214-1282 AD and the OSL age above the kiln constrains its burial to 1305-1445 AD, a possible relationship to the period of tremendous summer precipitation in the first half of the 14th century AD (e.g. Dotterweich, 2013; Herget et al., 2015) seems also feasible, either complementary or alternatively. But as indicated by the peat formation in NM-6, which was interrupted by pulses of colluvial sedimentation, it can be assumed, that incision of the gullies and detrital input into the 'Naugartener Moor' was dominantly triggered by alternating phases of prehistoric and later historic land use since the last 3200-2800 a. This is further supported by the occurrence of several archaeologically detected Slavic settlements in the close proximity (Supplement 2E).

5.2 Prehistoric and historic settlement history of the Quillow river catchment

As indicated by the occurrence of numerous archaeological findings (Figs. 1, 7), the study area has been populated since the Early Mesolithic (Terberger et al., 2004; Schulz, 2009). First agriculture was introduced into the upper Ucker river valley by the Linear Pottery Culture people (or communities) during the Early Neolithic around 7.3 to 7 ka BP (Schatz, 2000; Kulczycka-Leciejewiczowa and Wetzel, 2002). A widespread practice of arable farming occurred during the Middle Neolithic with the introduction of the wooden hook plough around 6.2 ka BP (Schulz, 2009). During the Early and Middle Neolithic, the study area was comparatively densely populated, followed by a decline of human impact around 3650 ± 250 a cal BP and a subsequent peak in the settlement density during the Late Bronze Age as reflected in pollen data from Lake Unteruckersee (Fig. 8; Jahns, 2001). For this period first evidence of human impact on the local environment is reported, e.g. deforestation (Jahns, 2000) and soil erosion inferred by colluvial sediments (Schulz, 2009). The subsequent decline of the population density in the Pre-Roman Iron Age is reflected in pollen data (Jahns, 2000) and in the archaeological record (Fig. 7; Schulz, 2009). During the Roman period the population increased again until the onset of the Migration period causing a widespread abandonment of the area (Schulz, 2009). In the beginning of the 8^{th} century AD the Uckermark region was colonised by Slavic tribes coming from the east. The so-called *Wendenkreuzzug* (Wendish Crusade) at 1147 AD ended the Slavic supremacy and initiated the German colonisation of that area (Enders, 1992; Kirsch, 2004; Schulz, 2009). In the 13^{th} century AD the population increased and the landscape was widely deforested. Catastrophic extreme weather events in the first half of the 14^{th} century AD led in conjunction with further crises such as the Black Death to a dramatic decline of the population density and an abandonment of nearly 25 % of the settlements and almost 50 % of the previous arable areas (Bork et al., 1998). Degraded top soils, animal diseases and crop failures led to a further decline of the population during the 15^{th} and 16^{th} centuries. In the late 16^{th} century AD the population and land use could be stabilised. This short period of prosperity ended with the Thirty Years' War (1618-1648 AD), causing massive devastation to the region including population losses of c. 90 % and the accompanying abandonment of fields and pastures (Enders, 1992). Population growth and economic prosperity in the 18^{th} and 19^{th} centuries AD called for the intensification of agriculture and further economic activities such as glassworks as well as charcoal, potash and tar production, leading to a massive decline of forested areas and the recultivation of agricultural land (Enders, 1992; Bleich, 2014).

As the histograms (Fig. 7), displaying the number of settlements for specific periods, show a similar distribution of settlements per archaeological period, a settlement index (number of settlements per reference area and archaeological period) was calculated to compare the compilations and to identify a potential bias in the settlement density of the respective area (Fig. 7A-B). Both histograms, however, show similar indices which indicate that the settlement history of the Quillow river catchment is representative even for the whole upper Ucker river catchment.

5.3 Late Holocene local land-use in palynological records

In the Uckermark region pollen records for the Late Holocene are generally rare (Jahns and Herking, 2002; Jahns, 2011). Only two ^{14}C-AMS-dated pollen diagrams showing the regional vegetation and land use development are available west and east of the study area (Fig. 1). The pollen diagram 'Unter-Ückersee' (UEC) of Jahns (2001; data available at the European Pollen Database, EPD; http://www.europeanpollendatabase.net) contains the period of 4700 to 1250 a cal BP with a high sample resolution of 4 to 29 samples per 1000 years. The chronology was taken from the EPD but recalculated for the section above the topmost radiocarbon date (2159-2001 a cal BP) by assuming, first, a constant rate of peat accumulation and, second, that 30 cm of peat have been lost from the top due to degradation after drainage (Jahns, 2001). The pollen diagram 'Carwitzer See' (CAR) spans the time period from 7000 a cal BP to the present with a sample resolution of 2 to 11 samples per 1000 years (Mrotzek 2017; Fig. 8).

First signs for Neolithic human impact become apparent after 5500 a cal BP in CAR where the Ulmus decline coincides with a slight increase in herbal pollen and the appearance of the pasture indicators Rumex acetosa type and Plantago lanceolata type (Fig. 8). At 4500 a cal BP the values of these indicators and of grasses (Wild grass group) increase, showing pasture activity until 2300 a cal BP. A single Cerealia pollen grain hint at arable land use only around 3100 a cal BP (late Bronze Age). The UEC record starts around 4700 a cal BP with already high values of pasture indicators accompanied by low Cerealia values, indicating arable farming during the late Neolithic. Values of anthropogenic indicators are lower after 4450 a cal BP and higher again between 3650 and 2630 a cal BP (Bronze Age).

At around 2300 a cal BP the indicators for pastoral and arable farming rise at UEC (pre-Roman Iron Age). After 2000 a cal BP stronger human impact is shown by higher values of herbal pollen and highest CEREALIA values indicating intensive arable farming until around 1780 a cal BP at UEC (Roman Iron Age).

The next signs for human activity are some CEREALIA pollen finds at CAR after 1550 a cal BP and the increase of herbal pollen and CEREALIA values at UEC after 1530 a cal BP. Whereas the anthropogenic indicator values remain low at CAR until 700 a cal BP, at UEC the high CEREALIA value of the uppermost sample indicate intensive arable farming around 1250 a cal BP (early Slavic). At CAR rising pasture activities are visible after 700 a cal BP. An increase of arable farming is apparent here after 350 a cal BP.

In general, the less distinct phases of human impact in the CAR record suggest weaker settlement activities in the hilly and more forested area around Lake Carwitzer See compared to the pronounced settlement phases derived from the UEC record which points at a more open landscape induced by human activity in the Ucker river valley.

The combination of palynological and archaeological records suggest that first arable farming in the Quillow river catchment dates to the Late Bronze Age in contrast to the Ucker river valley with its longer-lasting legacy of arable land use. It is, thus, proposed that from c. 4250 a cal BP onwards, land use – via soil erosion and translocation – leads to the colluvial layers in the profiles presented.

5.4 Comparing Late Holocene colluvial dynamics in Germany

The question arises as to what extent past soil erosion dynamics differ within the same region (i.e. in northeastern Germany) and, furthermore, as compared with other regions in Germany. After nearly two decades of intensive research on this matter, a broad base of geochronological data is available, now allowing for a meaningful discussion on this issue. In order to ensure methodical consistence, only studies applying luminescence dating were considered. With this approach a proper comparison of the colluvial sedimentation dynamics can be assured, as, alternatively, radiocarbon dates from organic material embedded in colluvial and alluvial sediments bear the potential of age overestimation (Alexandrovskiy & Chichagova, 1998; Wagner, 1998). Figure 9 shows the spatial distribution of dated sites in Germany, whereas Table 4 lists further information on these sites. In order to illustrate the temporal patterns, KDE plots were computed using published luminescence ages from colluvial layers (Fig. 10).

In northeastern Germany two further study areas with a sufficient number of dates exist. The area east of Lake Müritz shows a similar data distribution to the Quillow river catchment, whereas the East Brandenburg record comprises even older ages (Fig. 10A-C). The older peaks are ascribed to climatic forcing of Early Holocene soil erosion and shall not reflect human impact (Dreibrodt et al., 2010a). Nielsen et al. (2012) modelled the vegetation openness of northern Central Europe based on pollen data. They state for northeastern Germany a natural landscape openness of about 15-20 % at 8700 a, declining to 5-10 % at 6000 a. From 5200 a onwards, the dense forest cover declines due to human impact. At 3000 a the landscape openness amounts to 20-30 % (Nielsen et al., 2012).

In northeastern Germany the oldest colluvial sediments ascribed to human impact are reported from east Brandenburg with ages between 5300 and 7700 a. However, they were derived from a necropolis and shall not reflect colluvial layers produced by agriculture (Schatz, 2000). In the Lake Müritz region the oldest ages range between 3370 and 3970 a, which probably were produced by construction measures for a hill fortification in the Late Bronze Age instead of local agriculture (Küster et al., 2015). In the Quillow river catchment only one colluvial layer was dated to this period (STF2) and linked to agriculture of the Late Bronze Age.

Remarkably, although numerous Neolithic sites occur in northeast German study areas, no contemporary erosion-derived deposits were recorded. A reason for this could be a simple statistical phenomenon. The number of records and available datings is too small for their detection thus far. Certainly, the older the sediments, the lower their preservation potential. This specifically applies if the landscape investigated is an old cultural landscape with present-day intensive agriculture. Alternatively, Neolithic agriculture in the region may have been either performed without or with just little erosional imprint (e.g. livestock farming where grazing dominated) or, in case of arable farming, restricted to certain relief situations (e.g. flat areas) and very small fields that were not prone to erosion. Furthermore, no Neolithic settlements occur in the direct vicinity of our profiles, as this is the case in studies which present colluvial sediments connected with the Neolithic period (e.g. Lang et al., 2003b; Dreibrodt et al., 2013; Kittel, 2015).

A further argument for the missing of Neolithic colluvial sediments could be provided by the sediment cascade model introduced by Chorley et al. (1984) and later applied on colluvial sediments, for instance, by Lang and Hönscheidt (1999). It describes the pathway of sediments downslope, thereby passing several temporal sedimentary sinks. In succeeding erosion phases/events, older sediments from these sinks get remobilised and as a result the OSL-‘clock’ could have been reset. This might be a reason for the missing OSL ages up to 6-7 ka old, contrasting a pronounced occurrence of radiocarbon ages of this period from colluvial layers. In contrast, from southwest Germany even older colluvial sediments, which are ascribed to human-induced soil erosion with ages up to 11.2 ± 1.2 ka were reported (Lang et al., 2003b; Henkner et al. 2017; Fig. 10E). However, for some of these ages the possibility of insufficient bleaching during transport is discussed (Lang et al., 2003b). Indeed, the age compilation for this region is based mainly on studies concentrating on the (geo-) archaeology of Neolithic sites. Therefore, the chance to find and to date contemporary erosion-derived deposits is much higher in comparison to studies without such a focus (as in northeastern Germany). Pronounced maxima in the distribution of ages are correlated with the Late Bronze Age (4200-2800 a BP), the La Téne and Hallstatt Iron Age (2800-2100 a BP), the Roman period (2100-1700 a BP) and the Middle Ages (after 1300 a BP; Lang, 2003) .

Changing climatic conditions may also have contributed to the erosional dynamics reported in this study. Mayewski et al. (2004) compiled several phases of rapid climate change (RCC). Some RCC phases coincide with phases of enhanced soil erosion reconstructed from the presented OSL chronologies (Fig. 10). The oldest RCC phase at 9-8 ka is connected for Central Europe with a climate getting drier. This coincides with the findings of Dreibrodt et al. (2010) assuming for the oldest colluvia from Eastern Brandenburg (peak between 9-7.8 ka in Fig. 10C) cold and dry conditions with associated wildfires as the trigger for local soil erosion in the Early Holocene. The following RCC phases between 6-5 ka (cooling trend, becoming wetter) and 4.2-3.8 ka (warming trend) do not correlate clearly with the compiled KDE curves. In southern Germany (Fig. 10E) a larger number of datings (n = 14) fall into the RCC phase between 3.5-2.5 ka (cooling trend, becoming wetter). However, the increased occurrence of datings in this period is more likely connected to human impact (cf. Lang et al., 2003b). The same causal connection can be assumed for the RCC phase around 1.2-1 ka (cooling trend) and for the RCC phase from 0.6 ka onwards.

In the western German Hessen area Lang et al. (2003a) and Lang & Nolte (1999) dated a colluvial sequence interfingering with flood loams of the valley floor (Fig. 9; Tab. 4). Three distinct peaks appear at around 3.4 ka, 2.2 ka and c. 1.2 ka (Fig. 10-D). The two older peaks represent ages from several superimposed colluvial layers produced by farming (Lang et al., 2003a; Kühn et al., 2017), whereas the peak around 1 ka represents luminescence ages from flood plain fines of the same site.

Considering the rather large number of publications focussing on colluvial research in Germany it has to be noticed, that most of these studies are based on radiocarbon dating (e.g. Dotterweich, 2008; Dreibrodt et al., 2010b). These records often show chronologies reaching much further back in the past than studies based on optical dating. This is most likely related to the colluvial cascade effect as discussed above and due to the fact that embedded organic material (especially charcoal) can be reworked and redeposited to an unknown extent (e.g. Kühn et al., 2017). Furthermore, the lag between the time of death of the organism and its final embedding in a sediment layer is unknown and can only be used for the reconstruction of colluvial dynamics if a short time lag is assumed or proven (Wagner, 1998; Lang and Hönscheidt, 1999; Henkner et al., 2017).

What does this imply for the Quillow river catchment in northeastern Germany? The very distinct multimodal patterns of (prehistoric) peaks in the last 4000-5000 a observed in other study areas (Fig. 10B-E) cannot be confirmed for the Quillow river catchment. According to the datings, the last c. 600 a left a distinct imprint in the colluvial record. Generally, in northeastern Germany more than two third of all datings (total n = 91) fall within the last 800 a. This fact potentially proves the large-scale modification of a landscape by man in this region starting in the course of the medieval German colonisation and continuing afterwards, which is apparently later than in the central and southern part of Germany. Moreover, methodological effects have to be considered, such as different research aims of the works. Most of the studies in central and southern Germany were connected to geoarchaeological issues (e.g. Lang and Wagner, 1996; Lang and Hönscheidt, 1999; Lang et al., 2003b, Henkner et al., 2017), whereas in northeastern Germany pedo-stratigraphical questions have dominated so far (e.g. Küster et al., 2014; Kaiser et al., 2014; this study).

6 Conclusions

Knowledge on the spatial extent and temporal pattern of past colluvial deposition is needed to scale recently observed soil erosion in agricultural landscapes and to assist estimates about future trends of soil erosion.

The dating of colluvial sediments from different landforms in a mesoscale catchment of northeastern Germany using OSL and radiocarbon datings revealed a heterogeneous record of prehistoric and historic soil erosion. Several dated profiles located in differing landforms, such as lower slopes, kettle holes and gully systems, demonstrated the varying archive potential of these relief units. The simplest stratigraphies were found on slopes, whereas kettle holes exhibit highly differentiated sequences of colluvial layers and intercalated palaeosols.

In spite of numerous Neolithic settlements in the study area no correlative colluvial sediments were detected so far. First human-induced soil erosion is attributed to the Late Bronze Age, i.e. c. 4000 years ago. The luminescence ages of colluvial deposits of the Quillow river catchment and other sites in northeastern Germany reveal a more modern history of human-induced soil erosion, occurring dominantly in the last millennium. Most ages cluster within the last 600 years with a peak during the last 200 years, ascribing the main phase of local soil erosion to the recent past. By contrast, for the mid and southern part of Germany a pronounced two- or three-phased distribution of luminescence ages from colluvial sediments is apparent, dating back until the Early Neolithic.

Acknowledgements

This study was performed within the framework of the TERENO and ICLEA projects of the Helmholtz Association. The authors express their gratitude to Raphael Steup and Maike Schäbitz for assistance during fieldwork, to Detlef Deumlich and Wilfried Hierold for stimulating discussions in the field and to Gernot Verch for logistical support. The archaeological data for the Quillow river catchment and its surrounding were kindly provided by Mathias Schulz. We would like to thank Mary Teresa Lavin-Zimmer for improving the English and Piotr Kittel and two anonymous reviewers for their helpful comments.

References

Ad-hoc AG Boden, 2005. Bodenkundliche Kartieranleitung. Schweizerbart, Stuttgart.

Alexandrovskiy A.L., Chichagova O.A., 1998. The ^{14}C age of humic substances in palaeosols. Radiocarbon 40, 991–999.

Bertran, P., Texier, J.-P., 1999. Facies and microfacies of slope deposits. CATENA 35, 99-121.

Bleich, U., 2014. Teerofen und Schneidemühle bei Christianenhof, in: Mitteilungen des Uckermärkischen Geschichtsvereins zu Prenzlau 19, 48-55.

Bogena, H., Kunkel, R., Puetz, T., Vereecken, H., Kruger, E., Zacharias, S., Dietrich, P., Wollschlager, U., Kunstmann, H., Papen, H., Schmid, H.P., Munch, J.C., Priesack, E., Schwank, M., Bens, O., Brauer, A., Borg, E., Hajnsek, I., 2012. TERENO – Ein langfristiges Beobachtungsnetzwerk für die terrestrische Umweltforschung. Hydrologie und Wasserbewirtschaftung 56, 138-143.

Bogucki, P., 1996. The spread of early farming in Europe. American Scientist 84, 242-253.

Bork, H.R., Dalchow, C., Dotterweich, M., Schatz, T., Schmidtchen, G., 1998. Die Entwicklung der Landschaften Brandenburgs in den vergangenen Jahrtausenden, in: Klemm, V., Darkow, G., Bork, H.R. (Eds.), Geschichte der Landwirtschaft in Brandenburg. Mezogazda, Müncheberg, pp. 237-259.

Borówka, R.K., 1992. The pattern and magnitude of denudation in interplateau sedimentary basins during the Late Vistulian and Holocene. Wydawnictwo Naukowe Uniwersytetu im. Adama Mickiewica w Poznaniu, Seria Geografia 54, 1-177.

Brauer, A., Hajdas, I., Blockley, S.P.E., Bronk Ramsey, C., Christl, M., Ivy-Ochs, S., Moseley, G.E., Nowaczyk, N.N., Rasmussen, S.O., Roberts, H.M., Spötl, C., Staff, R.A., Svensson, A., 2014. The importance of independent chronology in integrating records of past climate change for the 60–8 ka INTIMATE time interval. Quaternary Science Reviews 106, 47-66.

Bronk Ramsey, C., 2009a. Bayesian analysis of radiocarbon dates. Radiocarbon 51, 337-360.

Chorley, R. J., Schumm, S.A., Sudgen, D.E., 1984. Geomorphology. Methuen, London.

Deumlich, D., Schmidt, R., Sommer, M., 2010. A multiscale soil–landform relationship in the glacial-drift area based on digital terrain analysis and soil attributes. Journal of Plant Nutrition and Soil Science 173, 843-851.

Dotterweich, M., 2008. The history of soil erosion and fluvial deposits in small catchments of Central Europe: Deciphering the long-term interaction between humans and the environment – A review. Geomorphology 101, 192-208.

Dotterweich, M., 2013. The history of human-induced soil erosion: Geomorphic legacies, early descriptions and research, and the development of soil conservation-A global synopsis. Geomorphology 201, 1-34.

Dotterweich, M., Schmitt, A., Schmidtchen, G., Bork, H.-R., 2003. Quantifying historical gully erosion in northern Bavaria. CATENA 50, 135-150.

Dreibrodt, S., Bork, H.-R., 2005. Historical soil erosion and landscape development at Lake Belau (North Germany) – a comparison of colluvial deposits and lake sediments. Zeitschrift für Geomorphologie, Supplementband 139, 101-128.

Dreibrodt, S., Jarecki, H., Lubos, C., Khamnueva, S.V., Klamm, M., Bork, H.-R., 2013. Holocene soil formation and soil erosion at a slope beneath the Neolithic earthwork Salzmünde (Saxony-Anhalt, Germany). CATENA 107, 1-14.

Dreibrodt, S., Lomax, J., Nelle, O., Lubos, C., Fischer, P., Mitusov, A., Reiss, S., Radtke, U., Nadeau, M., Grootes, P.M., Bork, H.-R., 2010a. Are mid-latitude slopes sensitive to climatic oscillations? Implications from an Early Holocene sequence of slope deposits and buried soils from eastern Germany. Geomorphology 122, 351-369.

Dreibrodt, S., Lubos, C., Terhorst, B., Damm, B., Bork, H.R., 2010b. Historical soil erosion by water in Germany: Scales and archives, chronology, research perspectives. Quaternary International 222, 80-95.

Duller, G.A., 2008. Luminescence Dating: guidelines on using luminescence dating in archaeology. English Heritage, Swindon.

Enders, L., 1992. Die Uckermark: Geschichte einer kurmärkischen Landschaft vom 12. bis zum 18. Jahrhundert. Böhlau, Weimar.

Fischer-Zujkov, U., Schmidt, R., Brande, A., 1999. Die Schwarzerden Nordostdeutschlands und ihre Stellung in der holozänen Landschaftsentwicklung. Journal of Plant Nutrition and Soil Science 162, 443-449.

Frielinghaus, M., Vahrson, W.-G., 1998. Soil translocation by water erosion from agricultural cropland into wet depressions (morainic kettle holes). Soil and Tillage Research 46, 23–30.

Fuchs, M., Fischer, M., Reverman, R., 2010. Colluvial and alluvial sediment archives temporally resolved by OSL dating: Implications for reconstructing soil erosion. Quaternary Geochronology 5, 269-273.

Galbraith, R.F., 2010. On plotting OSL equivalent doses. Ancient TL 28, 1-10.

Galbraith, R.F., Roberts, R.G., 2012. Statistical aspects of equivalent dose and error calculation and display in OSL dating: An overview and some recommendations. Quaternary Geochronology 11, 1-27.

Galbraith, R.F., Roberts, R.G., Laslett, G.M., Yoshida, H., Olley, J.M., 1999. Optical Dating of single and multiple grains of quartz from Jinmium rock shelter, northern Australia: Part I, Experimental design and statistical models. Archaeometry 41, 339-364.

Gramsch, B., 2000. Friesack: Letzte Jäger und Sammler in Brandenburg. in: Jahrbuch des Römisch-Germanischen Zentralmuseums Mainz 47, pp. 51–96.

Gronenborn, D., Strien, H.-C., Dietrich, S., Sirocko, F., 2014. ‘Adaptive cycles’ and climate fluctuations: a case study from Linear Pottery Culture in western Central Europe. Journal of Archaeological Science 51, 73-83.

Hardt, J., Böse, M., 2016. The timing of the Weichselian Pomeranian ice marginal position south of the Baltic Sea: A critical review of morphological and geochronological results. Quaternary International, in press, http://dx.doi.org/10.1016/j.quaint.2016.07.044.

Hardt, J., Lüthgens, C., Hebenstreit, R., Böse, M., 2016. Geochronological (OSL) and geomorphological investigations at the presumed Frankfurt ice marginal position in northeast Germany. Quaternary Science Reviews 154, 85-99.

Henkner, J., Ahlrichs, J.J., Downey, S., Fuchs, M., James, B.R., Knopf, T., Scholten, T., Teuber, S., Kühn, P., 2017. Archaeopedology and chronostratigraphy of colluvial deposits as a proxy for regional land use history (Baar, southwest Germany). CATENA 155, 93-113.

Herbrich, M., Gerke, H.H., Bens, O., Sommer, M., 2017. Water balance and leaching of dissolved organic and inorganic carbon of eroded Luvisols using high precision weighing lysimeters. Soil and Tillage Research 165, 144-160.

Herget, J., Kapala, A., Krell, M., Rustemeier, E., Simmer, C., Wyss, A., 2015. The millennium flood of July 1342 revisited. CATENA 130, 82-94.

Hoffmann, T., Schlummer, M., Notebaert, B., Verstraeten, G., Korup, O., 2013. Carbon burial in soil sediments from Holocene agricultural erosion, Central Europe. Global Biogeochemical Cycles 27, 828-835.

IUSS Working Group WRB, 2015. World reference base for soil resources 2014, update 2015. World Soil Resources Report No. 106. FAO, Rome.

Jahns, S., 2000. Late-glacial and Holocene woodland dynamics and land-use history of the Lower Oder valley, north-eastern Germany, based on two, AMS14C-dated, pollen profiles. Vegetation History and Archaeobotany 9, 111-123.

Jahns, S., 2001. On the Late Pleistocene and Holocene history of vegetation and human impact in the Ücker valley, north-eastern Germany. Vegetation History and Archaeobotany 10, 97-104.

Jahns, S., 2011. Die holozäne Waldgeschichte von Brandenburg und Berlin – eine aktuelle Übersicht. Tuexenia Beiheft 4, 47-55.

Jahns, S., Herking, C., 2002. Zur holozänen und spätpleistozänen Vegetationsgeschichte im westlichen unteren Odergebiet. in: Gringmuth-Dallmer, E., Leciejewicz, L. (Eds.), Forschungen zu Mensch und Umwelt im Odergebiet in ur- und frühgeschichtlicher Zeit. Philipp von Zabern, Mainz, pp. 33-49.

Janetzko, P., Schmidt, R., 2014. Norddeutsche Jungmoränenlandschaften, Handbuch der Bodenkunde. Wiley, 1-38.

Kaiser, K., Endtmann, E., Janke, W., 2000. Befunde zur Relief-, Vegetations- und Nutzungsgeschichte in Ackersöllen in Barth, Lkr. Nordvorpommern. Bodendenkmalpflege in Mecklenburg-Vorpommern 47, 151-180.

Kaiser, K., Lorenz, S., Germer, S., Juschus, O., Küster, M., Libra, J., Bens, O., Hüttl, R.F., 2012. Late Quaternary evolution of rivers, lakes and peatlands in northeast Germany reflecting past climatic and human impact–an overview. E & G - Quaternary Science Journal 61, 103-132.

Kaiser, K., Küster, M., Fülling, A., Theuerkauf, M., Dietze, E., Graventein, H., Koch, P.J., Bens, O., Brauer, A., 2014. Littoral landforms and pedosedimentary sequences indicating Late Holocene lake-level changes in northern central Europe - A case study from northeastern Germany. Geomorphology 216, 58-78.

Kalettka, T., Rudat, C., 2006. Hydrogeomorphic types of glacially created kettleholes in North-East Germany. Limnologica 36, 54–64.

Karasiewicz, M.T., Hulisz, P., Noryśkiewicz, A.M., Krześlak, I., Świtoniak, M., 2014. The record of hydroclimatic changes in the sediments of a kettle-hole in a young glacial landscape (north-central Poland). Quaternary International 328-329, 264-276.

Kirsch, K., 2004. Slawen und Deutsche in der Uckermark. Vergleichende Untersuchungen zur Siedlungsentwicklung vom 11. bis zum 14. Jahrhundert. Stuttgart.

Kittel, P., 2014. Slope deposits as an indicator of anthropopressure in the light of research in Central Poland. Quaternary International 324, 34-55.

Kittel, P., 2015. The prehistoric human impact on slope development at the archaeological site in Smólsk (Kuyavian Lakeland). Bulletin of Geography. Physical Geography Series 8, 107-122.

Kleber, A., 2006. "Kolluvium” does not equal “colluvium". Zeitschrift für Geomorphologie, NF 50, 541-542.

Kleeberg, A., Neyen, M., Schkade, U.-K., Kalettka, T., Lischeid, G., 2016. Sediment cores from kettle holes in NE Germany reveal recent impacts of agriculture. Environmental Science and Pollution Research 23, 7409-7424.

Klimek, K., 2010. Past and present interaction between the catchment and the valley floor: Upper Osoblaha basin, NE Sudetes slope and foreland. Quaternary International 220, 112-121.

Kulczycka-Leciejewiczowa, A., Wetzel, G., 2002. Neolithikum im Odergebiet,[w:] E. Gringmuth--Dallmer, L. Leciejewicz (red.), Forschungen zu Mensch und Umwelt im Odergebiet in urund frühgeschichtlicher Zeit, 257-270.

Kühn, P., Lehndorff, E., Fuchs, M., 2017. Lateglacial to Holocene pedogenesis and formation of colluvial deposits in a loess landscape of Central Europe (Wetterau, Germany). CATENA 154, 118-135.

Küster, M., Fülling, A., Kaiser, K., Ulrich, J., 2014. Aeolian sands and buried soils in the Mecklenburg Lake District, NE Germany: Holocene land-use history and pedo-geomorphic response. Geomorphology 211, 64-76.

Küster, M., Fülling, A., Ulrich, J., 2015. Bw horizon in Holocene slope deposits (Kratzeburg, NE Germany) – dating and pedological characteristics. E & G - Quaternary Science Journal 64, 111-117.

Küster, M., Ruchhöft, F., Lorenz, S., Janke, W., 2011. Geoarchaeological evidence of Holocene human impact and soil erosion on a till plain in Vorpommern (Kühlenhagen, NE-Germany). E & G - Quaternary Science Journal 60, 455-463.

Lang, A., 2003. Phases of soil erosion-derived colluviation in the loess hills of South Germany. CATENA 51, 209-221.

Lang, A., Wagner, G.A., 1996. Infrared stimulated luminescence dating of archaeosediments. Archaeometry 38, 129-141.

Lang, A., Hönscheidt, S., 1999. Age and source of colluvial sediments at Vaihingen–Enz, Germany. CATENA 38, 89-107.

Lang, A., Nolte, S., 1999. The chronology of Holocene alluvial sediments from the Wetterau, Germany, provided by optical and 14C dating. The Holocene 9, 207-214.

Lang, A., Bork, H.-R., Mäckel, R., Preston, N., Wunderlich, J., Dikau, R., 2003a. Changes in sediment flux and storage within a fluvial system: some examples from the Rhine catchment. Hydrological Processes 17, 3321-3334.

Lang, A., Niller, H.-P., Rind, M.M., 2003b. Land degradation in Bronze Age Germany: Archaeological, pedological, and chronometrical evidence from a hilltop settlement on the Frauenberg, Niederbayern. Geoarchaeology 18, 757-778.

Larsen, A., Bork, H.-R., Fuelling, A., Fuchs, M., Larsen, J.R., 2013. The processes and timing of sediment delivery from headwaters to the trunk stream of a Central European mountain gully catchment. Geomorphology 201, 215-226.

Leopold, M., Völkel, J., 2007. Colluvium: Definition, differentiation, and possible suitability for reconstructing Holocene climate data. Quaternary International 162-163, 133-140.

Lischeid, G., Kalettka, T., Holländer, M., Steidl, J., Merz, C., Dannowski, R., Hohenbrink, T., Lehr, C., Onandia, G., Reverey, F., Pätzig, M., 2017. Natural ponds in an agricultural landscape: External drivers, internal processes, and the role of the terrestrial-aquatic interface. Limnologica - Ecology and Management of Inland Waters, in press.

Lubos, C.C.M., Dreibrodt, S., Nelle, O., Klamm, M., Friederich, S., Meller, H., Nadeau, M.J., Grootes, P.M., Fuchs, M., Bork, H.R., 2011. A multi-layered prehistoric settlement structure (tell?) at Niederröblingen, Germany and its implications. Journal of Archaeological Science 38, 1101-1110.

Lubos, C.C.M., Dreibrodt, S., Robin, V., Nelle, O., Khamnueva, S., Richling, I., Bultmann, U., Bork, H.R., 2013. Settlement and environmental history of a multilayered settlement mound in Niederröblingen (central Germany) – a multi-proxy approach. Journal of Archaeological Science 40, 79-98.

Lüthgens, C., Böse, M., Preusser, F., 2011. Age of the Pomeranian ice-marginal position in northeastern Germany determined by Optically Stimulated Luminescence (OSL) dating of glaciofluvial sediments. Boreas 40, 598-615.

Mayewski, P.A., Rohling, E.E., Curt Stager, J., Karlén, W., Maasch, K.A., Meeker, L.D., Meyerson, E.A., Gasse, F., van Kreveld, S., Holmgren, K., Lee-Thorp, J., Rosqvist, G., Rack, F., Staubwasser, M., Schneider, R.R., Steig, E.J., 2004. Holocene Climate Variability. Quaternary Research 62, 243-255.

Miller, B., Juilleret, J., 2016. Defining Colluvium and Alluvium: An Experiment to Discuss and Consolidate Perspectives, EGU General Assembly Conference Abstracts, p. 17718.

Mrotzek, A., 2017. 34. Carwitzer See (north-eastern Germany): regional vegetation development during the past 7000 years. Grana, 318-320.

Murray, A.S., Wintle, A.G., 2000. Luminescence dating of quartz using an improved single-aliquot regenerative-dose protocol. Radiation Measurements 32, 57-73.

Nielsen, A.B., Giesecke, T., Theuerkauf, M., Feeser, I., Behre, K.-E., Beug, H.-J., Chen, S.-H., Christiansen, J., Dörfler, W., Endtmann, E., Jahns, S., de Klerk, P., Kühl, N., Latałowa, M., Odgaard, B.V., Rasmussen, P., Stockholm, J.R., Voigt, R., Wiethold, J., Wolters, S., 2012. Quantitative reconstructions of changes in regional openness in north-central Europe reveal new insights into old questions. Quaternary Science Reviews 47, 131-149.

Nitzsche, K.N., Kalettka, T., Premke, K., Lischeid, G., Gessler, A., Kayler, Z.E., 2017. Land-use and hydroperiod affect kettle hole sediment carbon and nitrogen biogeochemistry. Science of the Total Environment 574, 46-56.

Prescott, J.R., Hutton, J.T., 1988. Cosmic ray and gamma ray dosimetry for TL and ESR. International Journal of Radiation Applications and Instrumentation. Part D. Nuclear Tracks and Radiation Measurements 14, 223-227.

Prescott, J.R., Hutton, J.T., 1994. Cosmic ray contributions to dose rates for luminescence and ESR dating: Large depths and long-term time variations. Radiation Measurements 23, 497-500.

Pütz, T., Kiese, R., Wollschläger, U., Groh, J., Rupp, H., Zacharias, S., Priesack, E., Gerke, H.H., Gasche, R., Bens, O., Borg, E., Baessler, C., Kaiser, K., Herbrich, M., Munch, J.C., Sommer, M., Vogel, H.J., Vanderborght, J., Vereecken, H., 2016. TERENO-SOILCan: a lysimeter-network in Germany observing soil processes and plant diversity influenced by climate change. Environmental Earth Sciences 75, 1242.

Raab, A., Takla, M., Raab, T., Nicolay, A., Schneider, A., Rösler, H., Heußner, K.U., Bönisch, E., 2015. Pre-industrial charcoal production in Lower Lusatia (Brandenburg, Germany): Detection and evaluation of a large charcoal-burning field by combining archaeological studies, GIS-based analyses of shaded-relief maps and dendrochronological age determination. Quaternary International 367, 111-122.

Reimer, P.J., Bard, E., Bayliss, A., Beck, J.W., Blackwell, P.G., Ramsey, C.B., Buck, C.E., Cheng, H., Edwards, R.L., Friedrich, M., Grootes, P.M., Guilderson, T.P., Haflidason, H., Hajdas, I., Hatte, C., Heaton, T.J., Hoffmann, D.L., Hogg, A.G., Hughen, K.A., Kaiser, K.F., Kromer, B., Manning, S.W., Niu, M., Reimer, R.W., Richards, D.A., Scott, E.M., Southon, J.R., Staff, R.A., Turney, C.S.M., van der Plicht, J., 2013. Intcal13 and Marine13 Radiocarbon Age Calibration Curves 0-50,000 Years Cal Bp. Radiocarbon 55, 1869-1887.

Ryan, P., Blackford, J., 2010. Late Mesolithic environmental change at Black Heath, south Pennines, UK: a test of Mesolithic woodland man- agement models using pollen, charcoal and non-pollen palynomorph data. Vegetation History and Archaeobotany 19, 545–558.

Sanderson, D.C.W., Murphy, S., 2010. Using simple portable OSL measurements and laboratory characterisation to help understand complex and heterogeneous sediment sequences for luminescence dating. Quaternary Geochronology 5, 299-305.

Schatz, T., 2000. Untersuchungen zur holozänen Landschaftsentwicklung Nordostdeutschlands. ZALF, Müncheberg.

Schmettau, F.W.K. Graf von 1767. Schmettausches Kartenwerk 1767-1787, 1:50.000, Blatt 27, Landesvermessung und Geobasisinformation Brandenburg.

Schmitt, A., Rodzik, J., Zgłobicki, W., Russok, C., Dotterweich, M., Bork, H.-R., 2006. Time and scale of gully erosion in the Jedliczny Dol gully system, south-east Poland. CATENA 68, 124-132.

Schneider, T., 2014. Historischer Landnutzungswandel im Quillow-Einzugsgebiet in der Uckermark (Brandenburg) unter besonderer Berücksichtigung der Gemarkung Christianenhof und Umgebung. Bsc-Thesis, Hochschule für Nachhaltige Entwicklung Eberswalde, Eberswalde.

Schulz, M., 2009. Ur- und Frühgeschichte des Prenzlauer Raumes: von den Anfängen der menschlichen Besiedlung bis zu den Anfängen der Stadt im 13. Jahrhundert, in: Neitmann, K., Schich, W. (Eds.), Geschichte der Stadt Prenzlau. Geiger-Verlag, Horb am Neckar, pp. 15-26.

Sobietzky, G., 2009. Glashütten im Land Strelitz. Beiträge zur Glashüttenforschung 4, Stralsund.

Sommer, M., Gerke, H.H., Deumlich, D., 2008. Modelling soil landscape genesis - A ‘time split’ approach for hummocky agricultural landscapes. Geoderma 145, 480-493.

Strahl, J., 2010. Die Gliederung des Holozäns im Land Brandenburg, in: Landesamt für Bergbau, Geologie und Rohstoffe Brandenburg, 2010. Atlas zur Geologie von Brandenburg. Landesvermessung und Geobasisinformation Brandenburg, Potsdam, pp. 157.

Svizzero, S., 2015. Farmers’ spatial behaviour, demographic density dependence and the spread of Neolithic agriculture in Central Europe. Documenta Praehistorica 42, 133-146.

Szwarczewski, P., 2009. The formation of deluvial and alluvial cones as a consequence of human settlement on a loess plateau: an example from the Chroberz area (Poland). Radiocarbon 51, 445-455.

Terberger, T., De Klerk, P., Helbig, H., Kaiser, K., Kühn, P., 2004. Late Weichselian landscape development and human settlement in Mecklenburg-Vorpommern (NE Germany). Eiszeitalter und Gegenwart 54, 138-175.

Tinapp, C.H., Meller, H., Baumhauer, R., 2008. Holocene Accumulation of Colluvial and Alluvial Sediments in the Weiße Elster River Valley in Saxony, Germany. Archaeometry 50, 696-709.

Tolksdorf, J.F., Klasen, N., Hilgers, A., 2013. The existence of open areas during the Mesolithic: evidence from aeolian sediments in the Elbe–Jeetzel area, northern Germany. Journal of Archaeological Science 40, 2813-2823.

Twardy, J., 2011. Influences of man and climate changes on relief and geological structure transformation in Central Poland since the neolithic. Geographia Polonica 84 (Special Issue Part 1), 163-178.

Van Vliet-Lanoë, B., 1998. Frost and soils: implications for paleosols, paleoclimates and stratigraphy. CATENA 34, 157-183.

Vanwalleghem, T., Gómez, J.A., Infante Amate, J., González de Molina, M., Vanderlinden, K., Guzmán, G., Laguna, A., Giráldez, J.V., 2017. Impact of historical land use and soil management change on soil erosion and agricultural sustainability during the Anthropocene. Anthropocene 17, 13-29.

Vermeesch, P., 2012. On the visualisation of detrital age distributions. Chemical Geology 312–313, 190-194.

Vogt, R., 2014. Kolluvien als Archive für anthropogen ausgelöste Landschaftsveränderungen an Beispielen aus der westlichen Bodenseeregion (Materialhefte zur Archäologie in Baden-Württemberg). Konrad-Theiss Verlag, Darmstadt.

Wagner, G.A., 1998. Age determination of young rocks and artifacts: physical and chemical clocks in quaternary geology and archaeology. Springer Verlag Berlin Heidelberg, Heidelberg.

Walker, M.J.C., Berkelhammer, M., Björck, S., Cwynar, L.C., Fisher, D.A., Long, A.J., Lowe, J.J., Newnham, R.M., Rasmussen, S.O., Weiss, H., 2012. Formal subdivision of the Holocene Series/Epoch: a Discussion Paper by a Working Group of INTIMATE (Integration of ice-core, marine and terrestrial records) and the Subcommission on Quaternary Stratigraphy (International Commission on Stratigraphy). Journal of Quaternary Science 27, 649-659.

Wilken, F., Sommer, M., Van Oost, K., Bens, O., Fiener, P., 2017. Process-oriented modelling to identify main drivers of erosion-induced carbon fluxes. SOIL 3, 83-94.

Wulf, M., Jahn, U., Meier, K., 2016. Land cover composition determinants in the Uckermark (NE Germany) over a 220-year period. Regional Environmental Change 16, 1793-1805.

Zacharias, S., Bogena, H., Samaniego, L., Mauder, M., Fuß, R., Pütz, T., Frenzel, M., Schwank, M., Baessler, C., Butterbach-Bahl, K., Bens, O., Borg, E., Brauer, A., Dietrich, P., Hajnsek, I., Helle, G., Kiese, R., Kunstmann, H., Klotz, S., Munch, J.C., Papen, H., Priesack, E., Schmid, H.P., Steinbrecher, R., Rosenbaum, U., Teutsch, G., Vereecken, H., 2011. A Network of Terrestrial Environmental Observatories in Germany. Vadose Zone Journal 10, 955.

Zádorová, T., Penížek, V., Šefrna, L., Drábek, O., Mihaljevič, M., Volf, Š., Chuman, T., 2013. Identification of Neolithic to Modern erosion–sedimentation phases using geochemical approach in a loess covered sub-catchment of South Moravia, Czech Republic. Geoderma 195–196, 56-69.

Zolitschka, B., Behre, K.-E., Schneider, J., 2003. Human and climate impact on the environment as derived from colluvial, fluvial and lacustrine archives - examples from the Bronze Age to the Migration period, Germany. Quaternary Science Reviews 22, 81-100.

Figures

Fig. 1: Map of the Quillow river catchment, distribution of archaeological sites and investigated profiles. Investigated sites (with soil profile ID): 1: Lake Tiefer See (TSU09, TSU17); 2: Steinfurth (STF2, STF3); 3: Falkenhagen (FKHG1); 4: Falkenhagen (FKHG2); 5: Naugarten (NAU11, NAU13, NM-6); 6: Christianenhof (CHRIST647); 7: Christianenhof (CHRIST1); 8: Raakow (RAAK1); 9: Raakow (RAAK2); 10: Grauenhagen (GRHG1).

Fig. 2: Photographs of the investigated profiles and photorealistic drawing of core NM6.

Fig. 3: Simplified pedological and sedimentological logs including geochronology of all investigated profiles.

Fig. 4: Physical and chemical properties of the colluvial sediment samples analysed. A: Ternary diagram showing textural classes of the colluvial sediment samples analysed (classification after FAO, 2006). B: Box plot showing the TOC content of the colluvial sediment samples analysed.

Fig. 5: Kernel Density Estimates of all OSL ages obtained from colluvial layers in the Quillow river catchment.

Fig. 6: Scaled sketch of an excavated trench at the footslope of the kettle hole at section Steinfurth (STF).

Fig. 7: Histograms of prehistoric and historic settlements. A: Upper Ucker river catchment. B: Quillow river catchment. Numbers on top of the bars represent the settlement index (Numbers of settlements per reference area [km^2]) for the respective archaeological period. Chronology of the cultural periods according to Strahl et al. (2010). C: Kernel Density Estimate from all colluvial layers in the Quillow river catchment.

Fig. 8: Selected pollen types from the pollen diagrams Carwitzer See (Mrotzek, 2017) and Unter-Ückersee (Jahns, 2001) indicating human-induced vegetation changes in the Late Holocene. Red stars represent age control by radiocarbon dating.

Fig. 9: Map of sites contributing to the Kernel Density Estimates shown in Figure 9.

Fig. 10: Kernel Density Estimates of OSL ages from colluvial layers obtained from several regions in Germany. See Table 4 for the studies contributing the data. Green shaded bars indicate phases of rapid climate change (RCC) after Mayewski et al. (2004).

Tables

Tab. 1: Sedimentological data of the investigated profiles.

Tab. 2: Optical stimulated luminescence data; dosimetry data, equivalent doses (ED) and OSL ages.

Tab. 3: Radiocarbon data of the investigated profiles.

Tab. 4: List of case studies contributing the ages to the Kernel Density Estimates of Figure 10.

Supplementary material

Supplement 1: Geological map of the study area with the main lithological units (General Geological Map of the Federal Republic of Germany 1:200000, Sheet CC 3142, Neubrandenburg).

Supplement 2: Maps showing the relief situation around the profiles analysed using a 1 m-LiDaR-DEM (Federal State of Brandenburg) derived colour-coded hillshade model (A-H). I: At the site TSU, no 1 m-LiDaR data were available and a 10 m-DEM derived colour-coded hillshade model was used. Orange square: Bronze Age settlement; green dot: Neolithic settlement; pink pentagon: Slavic settlement; red-black cross in circle: Roman Age settlement.

Supplement 3: De-distributions of all OSL ages obtained in this study.

Supplement 4: Geological map of the study area with the main lithological units (General Geological Map of the Federal Republic of Germany 1:200000, Sheet CC 3142, Neubrandenburg) and the archeological settlements (data kindly provided by M. Schulz).

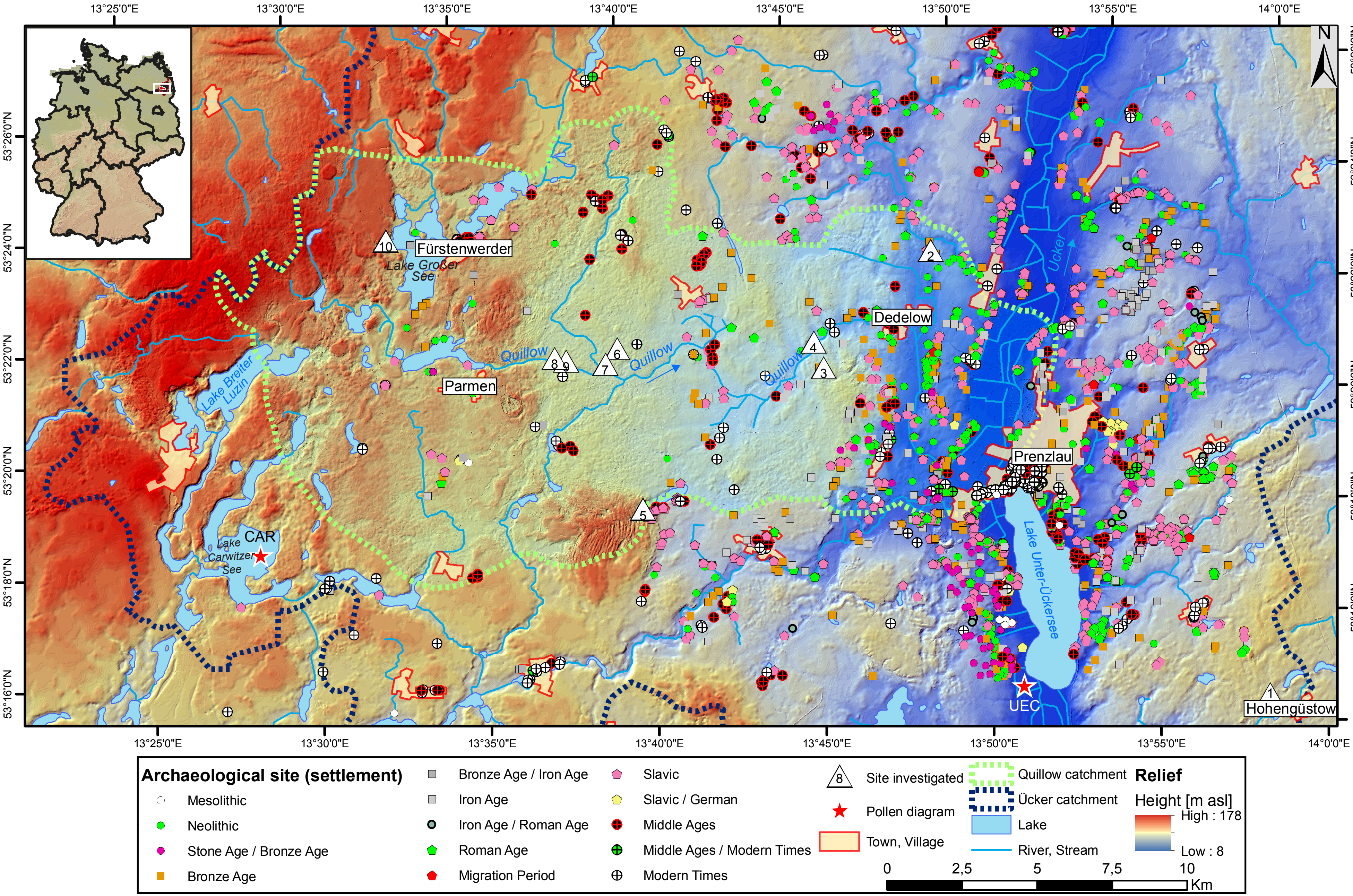

13°25'0"E
13°30'0"E
13°35'0"E
13°40'0"E
13°45'0"E
13°50'0"E
13°55'0"E
14°0'0"E
53°26'0"N
53°24'0"N
53°22'0"N
53°20'0"N
53°18'0"N
53°16'0"N
N
Fürstenwerder
Lake Großer See
Dedelow
Parmen
Prenzlau
Quillow
Ucker
Lake Breiter Luzin
CAR
Lake Carwitzer See
Lake Unter-Ückersee
UEC
Hohengüstow
Archaeological site (settlement)
Mesolithic
Neolithic
Stone Age / Bronze Age
Bronze Age
Bronze Age / Iron Age
Iron Age
Iron Age / Roman Age
Roman Age
Migration Period
Slavic
Slavic / German
Middle Ages
Middle Ages / Modern Times
Modern Times
Site investigated
Pollen diagram
Town, Village
Quillow catchment
Ücker catchment
Lake
River, Stream
Relief
Height [m asl]
High : 178
Low : 8
0
2,5
5
7,5
10
Km

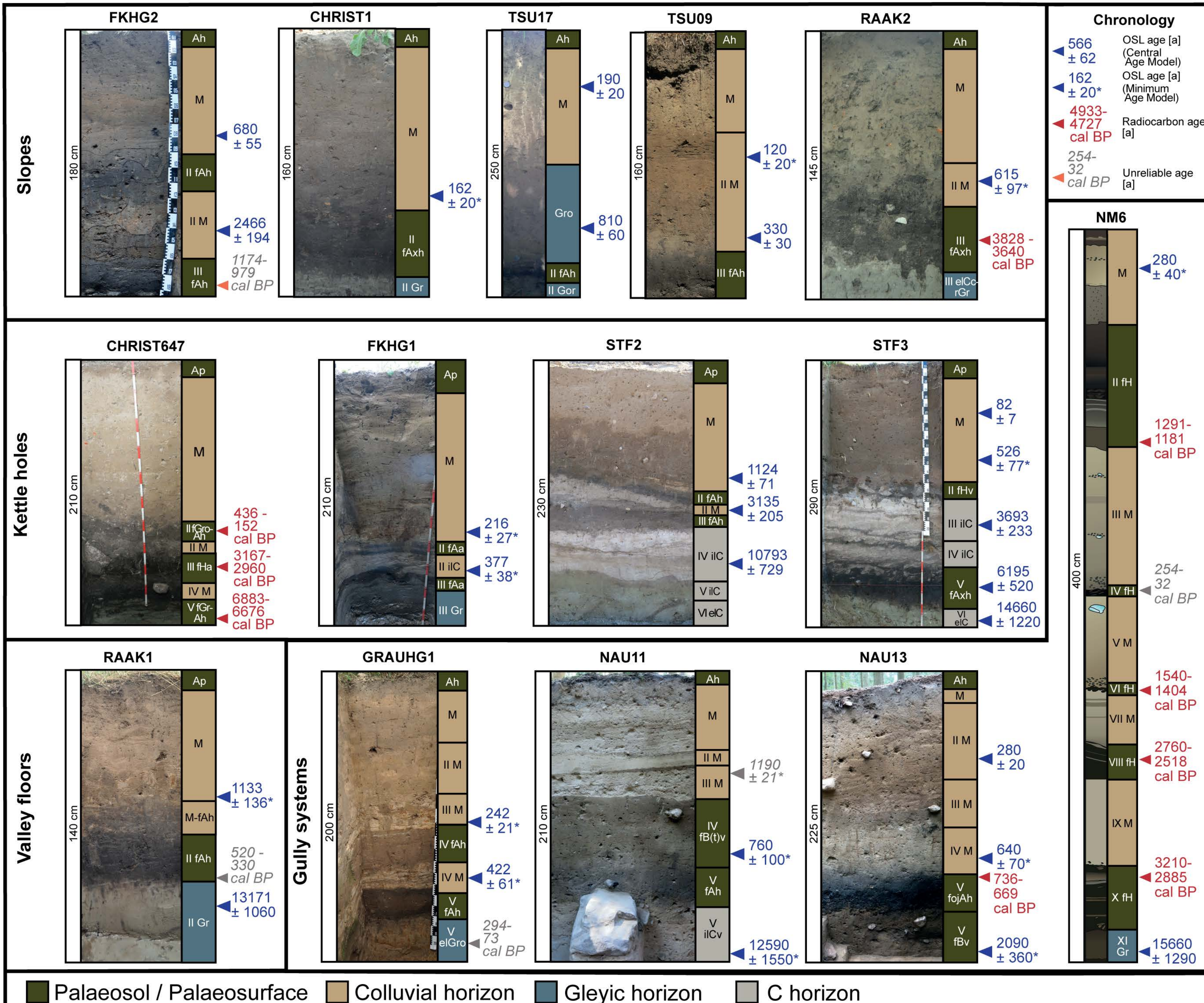
Slopes
FKHG2
180 cm
Ah
M
II fAh
II M
III fAh
680 ± 55
2466 ± 194
1174-979 cal BP
CHRIST1
160 cm
Ah
M
II fAxh
II Gr
162 ± 20*
TSU17
250 cm
Ah
M
Gro
II fAh
II Gor
190 ± 20
810 ± 60
TSU09
160 cm
Ah
M
II M
III fAh
120 ± 20*
330 ± 30
RAAK2
145 cm
Ah
M
II M
III fAxh
III elCc-rGr
615 ± 97*
3828 - 3640 cal BP
Chronology
566 ± 62
OSL age [a] (Central Age Model)
162 ± 20*
OSL age [a] (Minimum Age Model)
4933-4727 cal BP
Radiocarbon age [a]
254-32 cal BP
Unreliable age [a]
Kettle holes
CHRIST647
210 cm
Ap
M
II fGro-Ah
II M
III fHa
IV M
V fGr-Ah
436 - 152 cal BP
3167-2960 cal BP
6883-6676 cal BP
FKHG1
210 cm
Ap
M
II fAa
II ilC
III fAa
III Gr
216 ± 27*
377 ± 38*
STF2
230 cm
Ap
M
II fAh
II M
III fAh
IV ilC
V ilC
VI elC
1124 ± 71
3135 ± 205
10793 ± 729
STF3
290 cm
Ap
M
II fHv
III ilC
IV ilC
V fAxh
VI elC
82 ± 7
526 ± 77*
3693 ± 233
6195 ± 520
14660 ± 1220
NM6
400 cm
M
II fH
III M
IV fH
V M
VI fH
VII M
VIII fH
IX M
X fH
XI Gr
280 ± 40*
1291-1181 cal BP
254-32 cal BP
1540-1404 cal BP
2760-2518 cal BP
3210-2885 cal BP
15660 ± 1290
Valley floors
RAAK1
140 cm
Ap
M
M-fAh
II fAh
II Gr
1133 ± 136*
520 - 330 cal BP
13171 ± 1060
Gully systems
GRAUHG1
200 cm
Ah
M
II M
III M
IV fAh
IV M
V fAh
V elGro
242 ± 21*
422 ± 61*
294-73 cal BP
NAU11
210 cm
Ah
M
II M
III M
IV fB(t)v
V fAh
V ilCv
1190 ± 21*
760 ± 100*
12590 ± 1550*
NAU13
225 cm
Ah
M
II M
III M
IV M
V fojAh
V fBv
280 ± 20
640 ± 70*
736-669 cal BP
2090 ± 360*
Palaeosol / Palaeosurface
Colluvial horizon
Gleyic horizon
C horizon

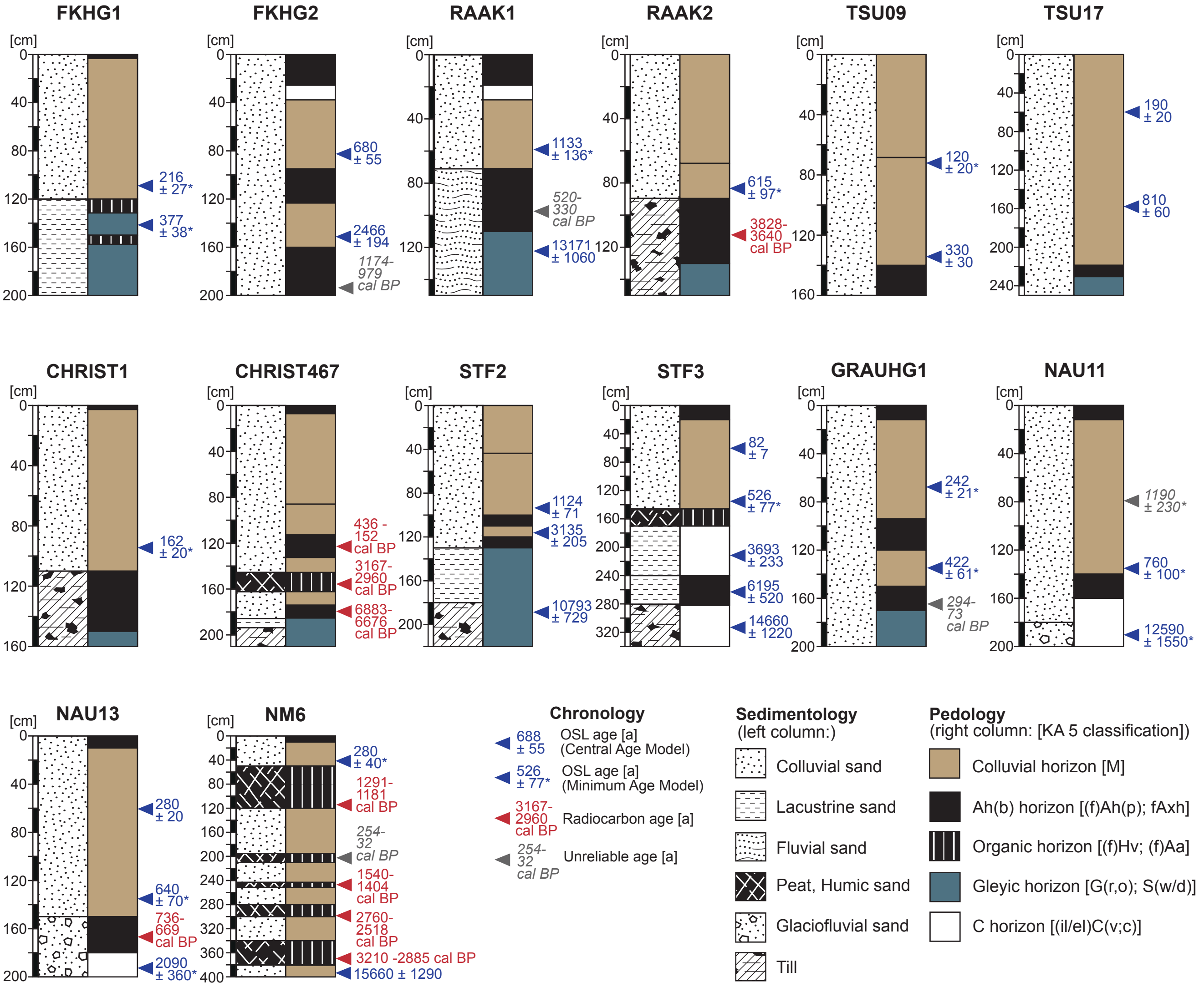
FKHG1
FKHG2
RAAK1
RAAK2
TSU09
TSU17
CHRIST1
CHRIST467
STF2
STF3
GRAUHG1
NAU11
NAU13
NM6
[cm]
216 ± 27*
377 ± 38*
680 ± 55
2466 ± 194
1174-979 cal BP
1133 ± 136*
520-330 cal BP
13171 ± 1060
615 ± 97*
3828-3640 cal BP
120 ± 20*
330 ± 30
190 ± 20
810 ± 60
162 ± 20*
436 - 152 cal BP
3167-2960 cal BP
6883-6676 cal BP
1124 ± 71
3135 ± 205
10793 ± 729
82 ± 7
526 ± 77*
3693 ± 233
6195 ± 520
14660 ± 1220
242 ± 21*
422 ± 61*
294-73 cal BP
1190 ± 230*
760 ± 100*
12590 ± 1550*
280 ± 20
640 ± 70*
736-669 cal BP
2090 ± 360*
280 ± 40*
1291-1181 cal BP
254-32 cal BP
1540-1404 cal BP
2760-2518 cal BP
3210 -2885 cal BP
15660 ± 1290
Chronology
688 ± 55 OSL age [a] (Central Age Model)
526 ± 77* OSL age [a] (Minimum Age Model)
3167-2960 cal BP Radiocarbon age [a]
254-32 cal BP Unreliable age [a]
Sedimentology (left column:)
Colluvial sand
Lacustrine sand
Fluvial sand
Peat, Humic sand
Glaciofluvial sand
Till
Pedology (right column: [KA 5 classification])
Colluvial horizon [M]
Ah(b) horizon [(f)Ah(p); fAxh]
Organic horizon [(f)Hv; (f)Aa]
Gleyic horizon [G(r,o); S(w/d)]
C horizon [(il/el)C(v;c)]

A

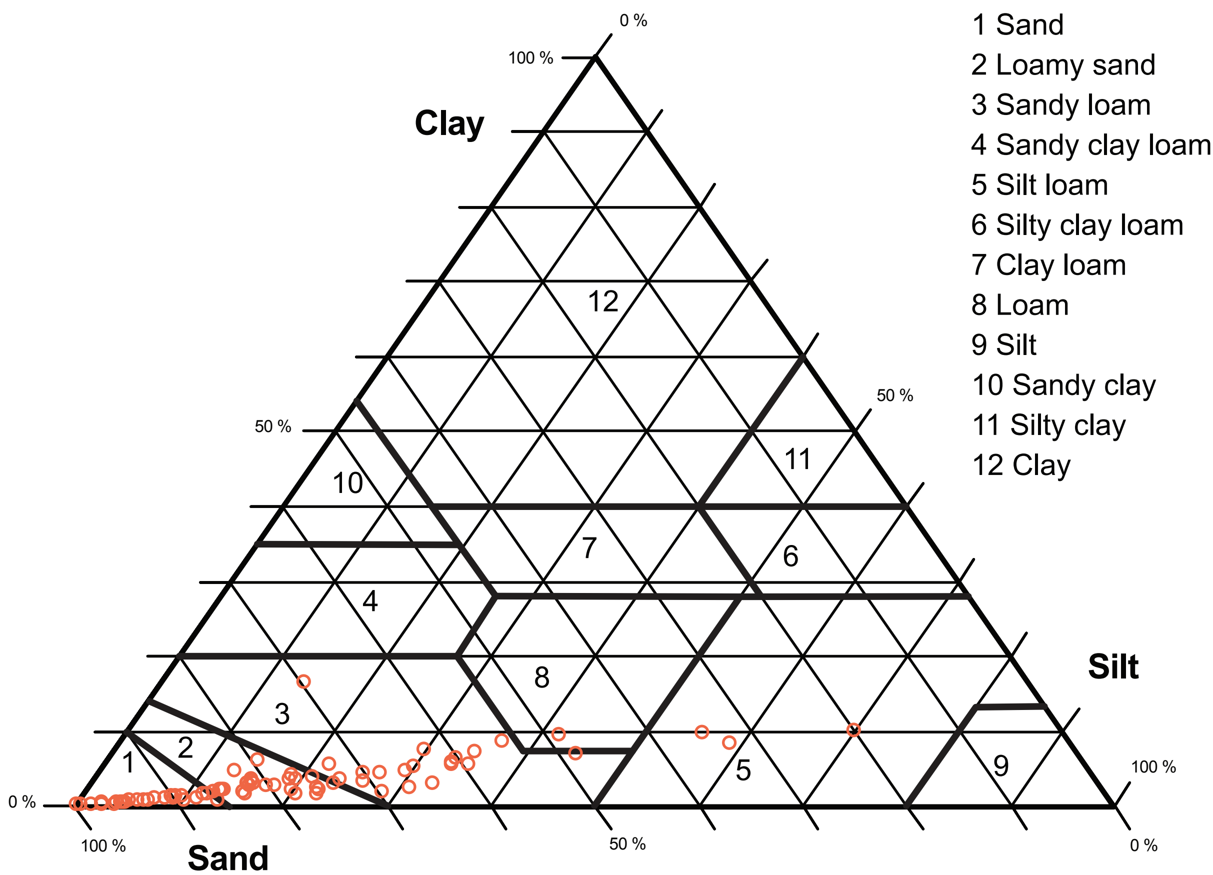

0 %
100 %
Clay
50 %
50 %
0 %
100 %
Silt
100 %
Sand
50 %
0 %
1
2
3
4
5
6
7
8
9
10
11
12
1 Sand
2 Loamy sand
3 Sandy loam
4 Sandy clay loam
5 Silt loam
6 Silty clay loam
7 Clay loam
8 Loam
9 Silt
10 Sandy clay
11 Silty clay
12 Clay

B

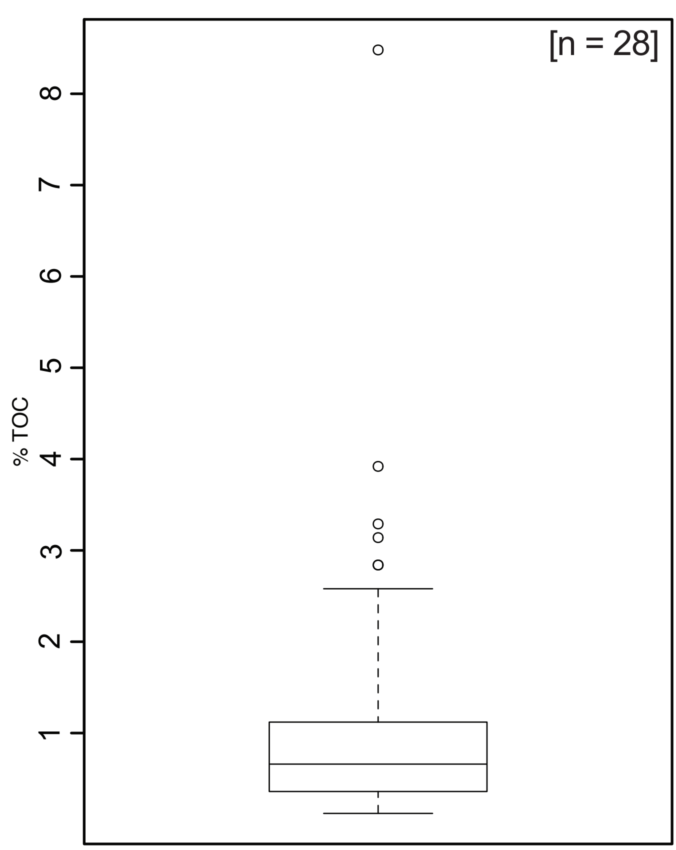

[n = 28]
% TOC
1
2
3
4
5
6
7
8

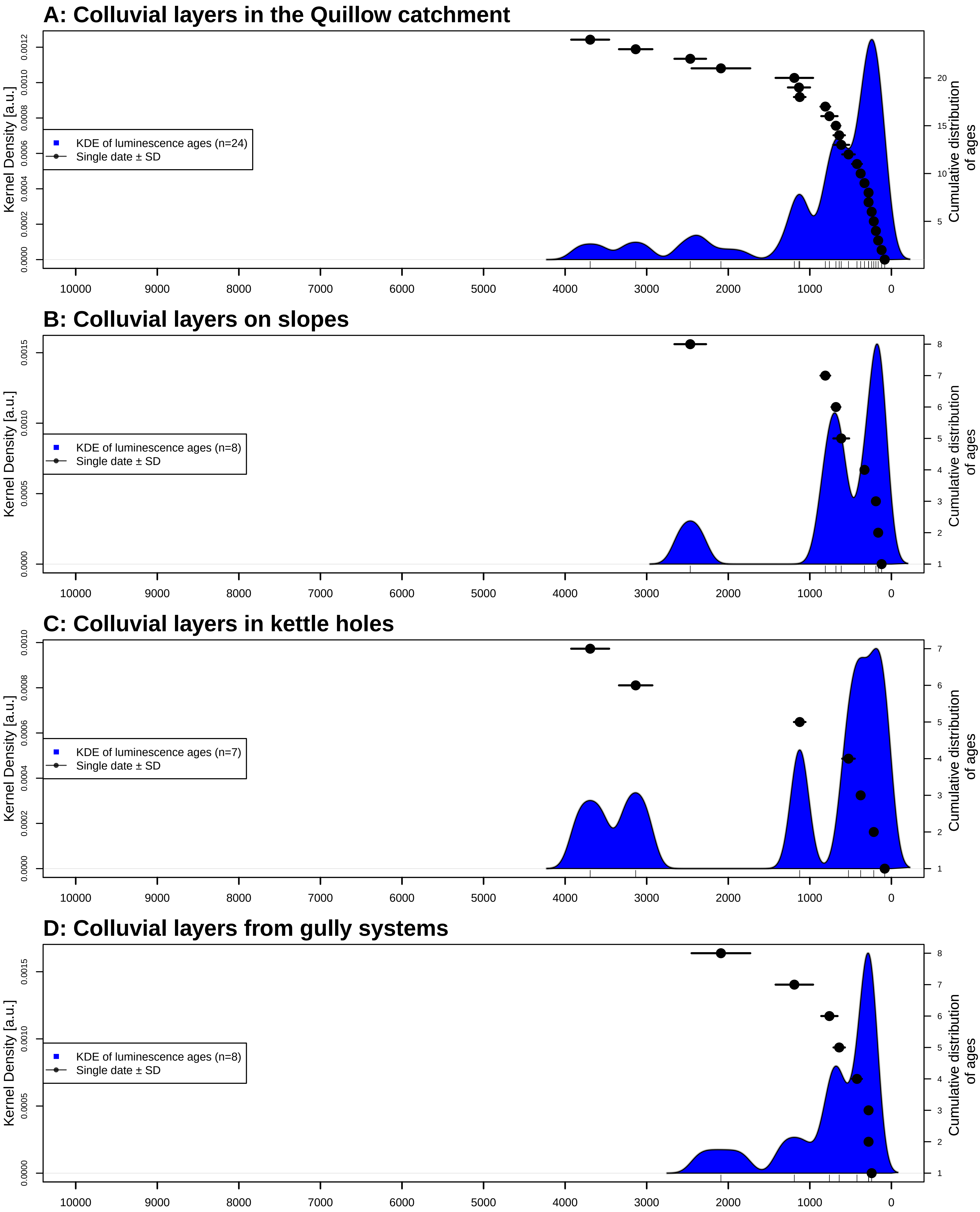
A: Colluvial layers in the Quillow catchment
KDE of luminescence ages (n=24)
Single date ± SD
Kernel Density [a.u.]
Cumulative distribution of ages
0.0000
0.0002
0.0004
0.0006
0.0008
0.0010
0.0012
5
10
15
20
10000
9000
8000
7000
6000
5000
4000
3000
2000
1000
0
B: Colluvial layers on slopes
KDE of luminescence ages (n=8)
Single date ± SD
Kernel Density [a.u.]
Cumulative distribution of ages
0.0000
0.0005
0.0010
0.0015
1
2
3
4
5
6
7
8
10000
9000
8000
7000
6000
5000
4000
3000
2000
1000
0
C: Colluvial layers in kettle holes
KDE of luminescence ages (n=7)
Single date ± SD
Kernel Density [a.u.]
Cumulative distribution of ages
0.0000
0.0002
0.0004
0.0006
0.0008
0.0010
1
2
3
4
5
6
7
10000
9000
8000
7000
6000
5000
4000
3000
2000
1000
0
D: Colluvial layers from gully systems
KDE of luminescence ages (n=8)
Single date ± SD
Kernel Density [a.u.]
Cumulative distribution of ages
0.0000
0.0005
0.0010
0.0015
1
2
3
4
5
6
7
8
10000
9000
8000
7000
6000
5000
4000
3000
2000
1000
0

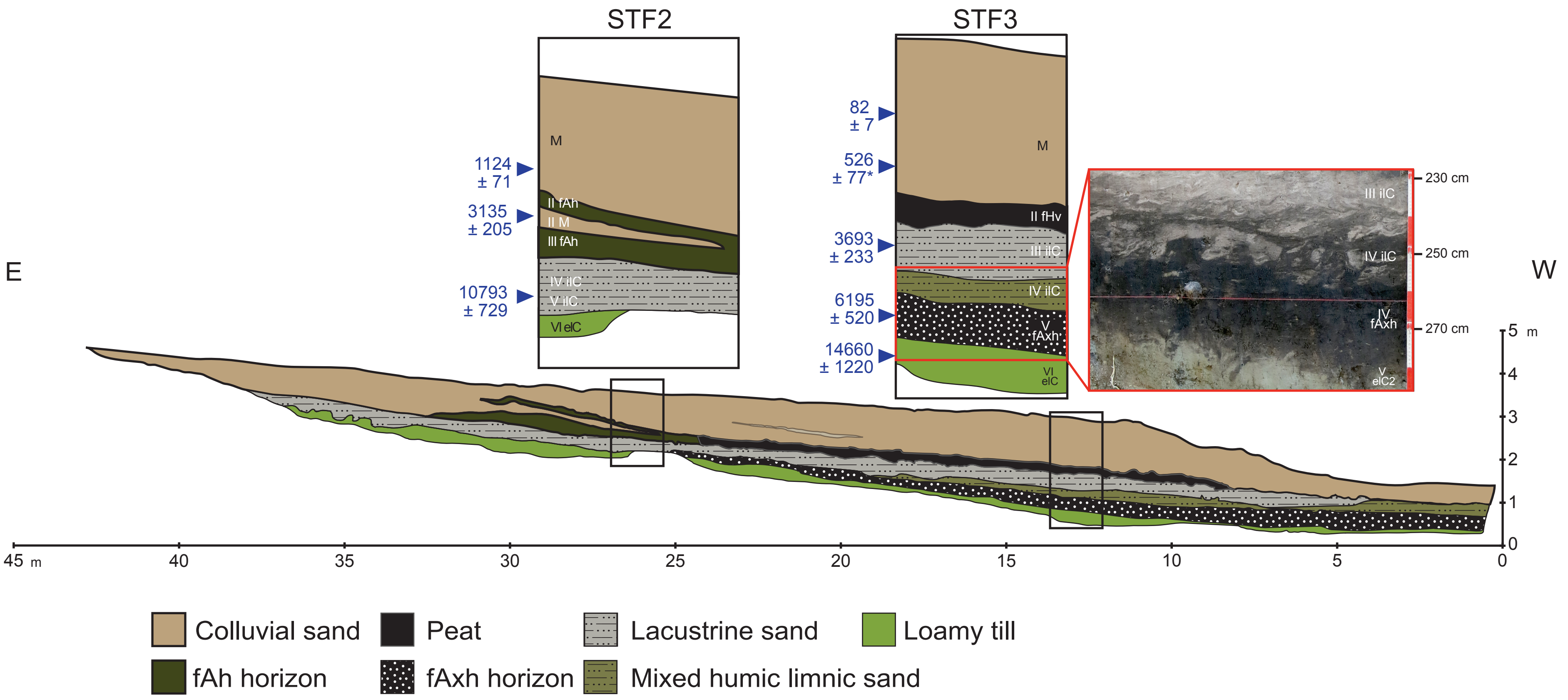

STF2
STF3
M
1124 ± 71
II fAh
II M
3135 ± 205
III fAh
IV ilC
V ilC
10793 ± 729
VI elC
82 ± 7
526 ± 77*
II fHv
3693 ± 233
III ilC
IV ilC
6195 ± 520
V fAxh
14660 ± 1220
VI elC
III ilC
IV ilC
IV fAxh
V elC2
230 cm
250 cm
270 cm
E
W
5 m
4
3
2
1
0
45 m
40
35
30
25
20
15
10
5
0
Colluvial sand
Peat
Lacustrine sand
Loamy till
fAh horizon
fAxh horizon
Mixed humic limnic sand

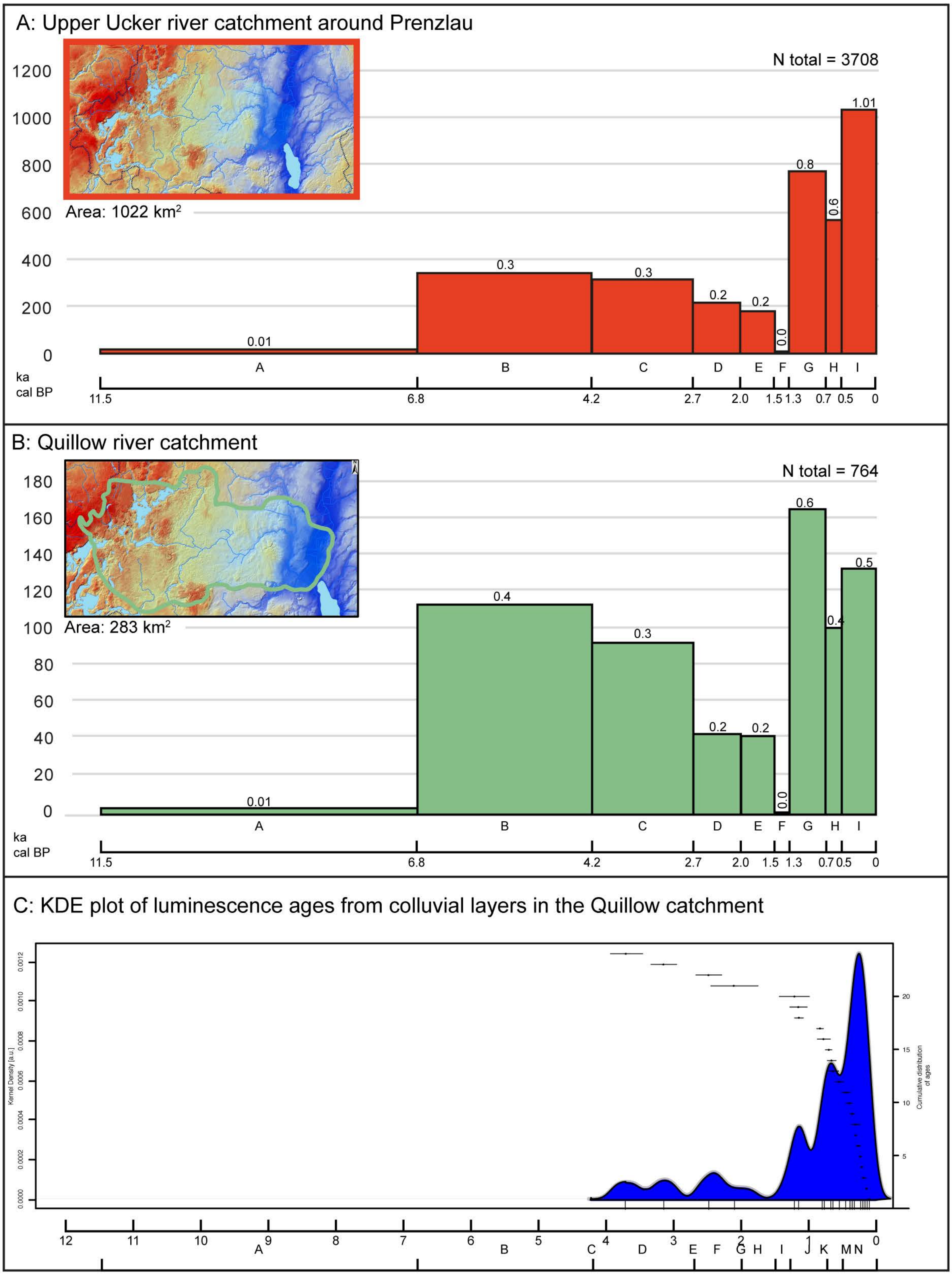

A - Mesolithic
B - Neolithic
C - Bronze Age
D - Iron Age
E - Roman Age
F - Migration period
G - Slavic
H - High Middle Ages
I - Modern period

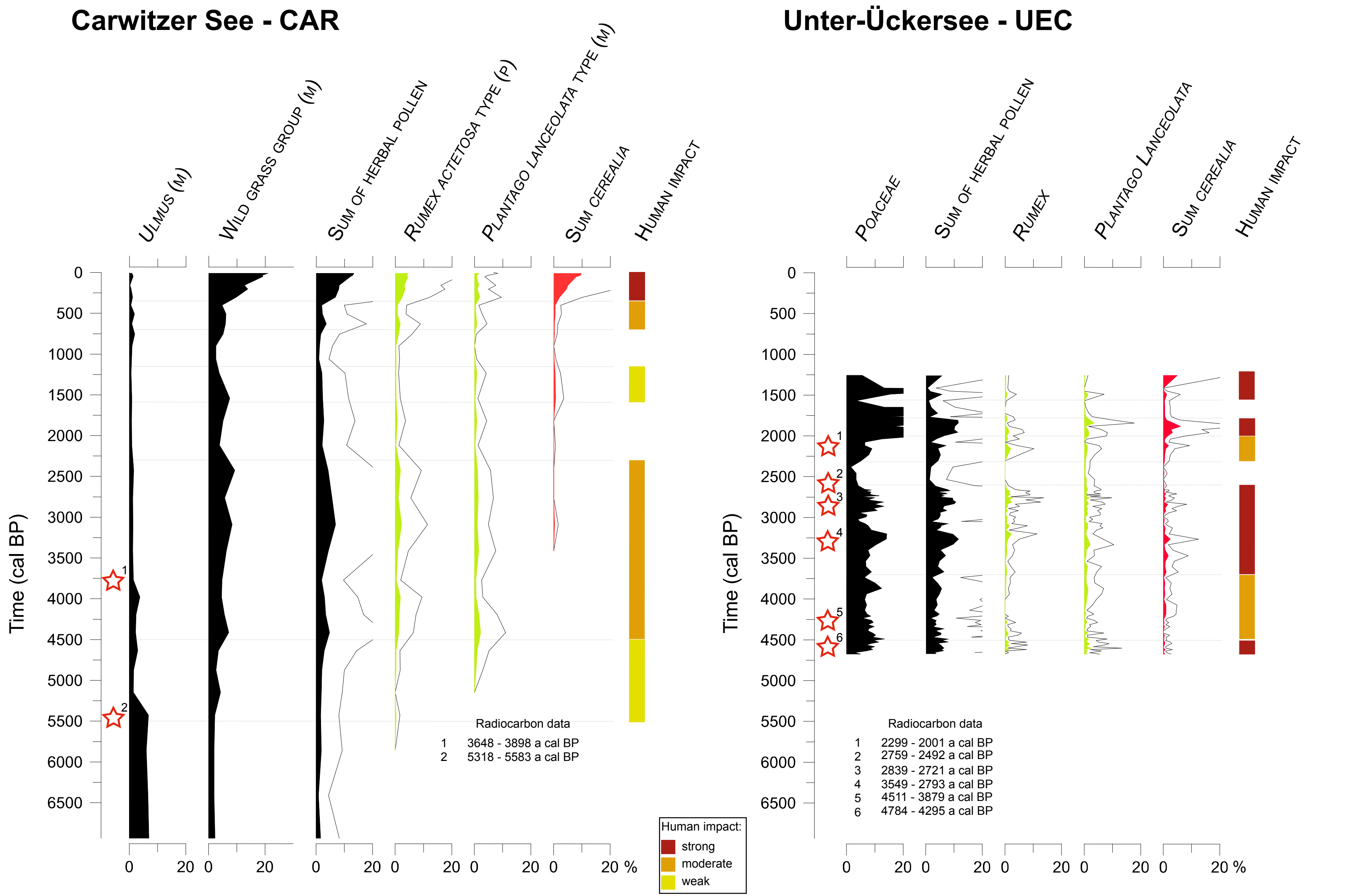

Carwitzer See - CAR
Unter-Ückersee - UEC
Ulmus (M)
Wild grass group (M)
Sum of herbal pollen
Rumex acetosa type (P)
Plantago lanceolata type (M)
Sum cerealia
Human impact
Poaceae
Sum of herbal pollen
Rumex
Plantago lanceolata
Sum cerealia
Human impact
Time (cal BP)
0
500
1000
1500
2000
2500
3000
3500
4000
4500
5000
5500
6000
6500
0 20 0 20 0 20 0 20 0 20 0 20 %
Radiocarbon data
1 3648 - 3898 a cal BP
2 5318 - 5583 a cal BP
Radiocarbon data
1 2299 - 2001 a cal BP
2 2759 - 2492 a cal BP
3 2839 - 2721 a cal BP
4 3549 - 2793 a cal BP
5 4511 - 3879 a cal BP
6 4784 - 4295 a cal BP
Human impact:
strong
moderate
weak

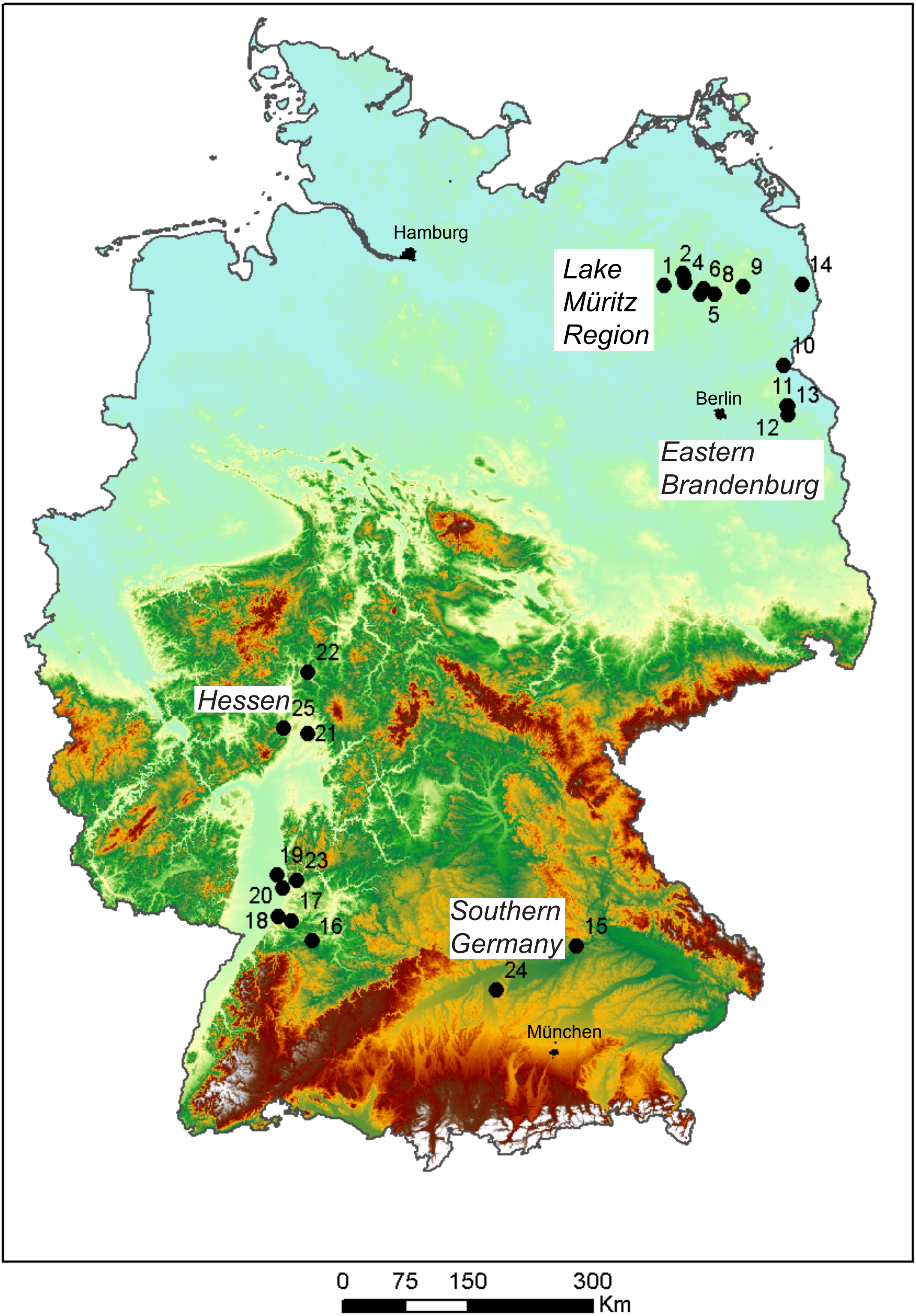

Hamburg
Lake
Müritz
Region
1
2
4
6
8
9
14
5
10
11
13
12
Berlin
Eastern
Brandenburg
22
Hessen
25
21
19
23
20
17
18
16
Southern
Germany
15
24
München
0
75
150
300
Km

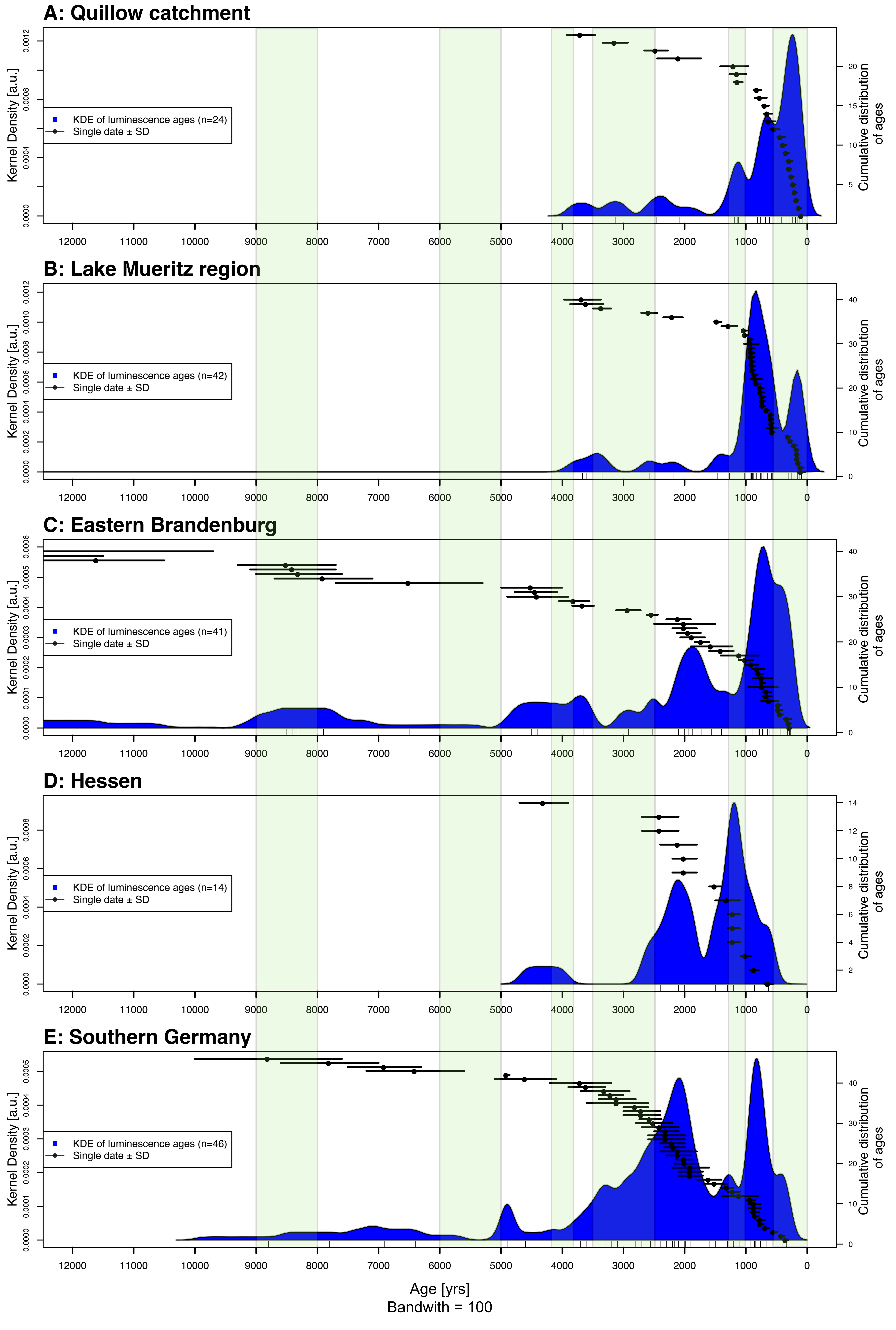

A: Quillow catchment
B: Lake Mueritz region
C: Eastern Brandenburg
D: Hessen
E: Southern Germany
KDE of luminescence ages (n=24)
KDE of luminescence ages (n=42)
KDE of luminescence ages (n=41)
KDE of luminescence ages (n=14)
KDE of luminescence ages (n=46)
Single date ± SD
Kernel Density [a.u.]
Cumulative distribution of ages
Age [yrs]
Bandwith = 100

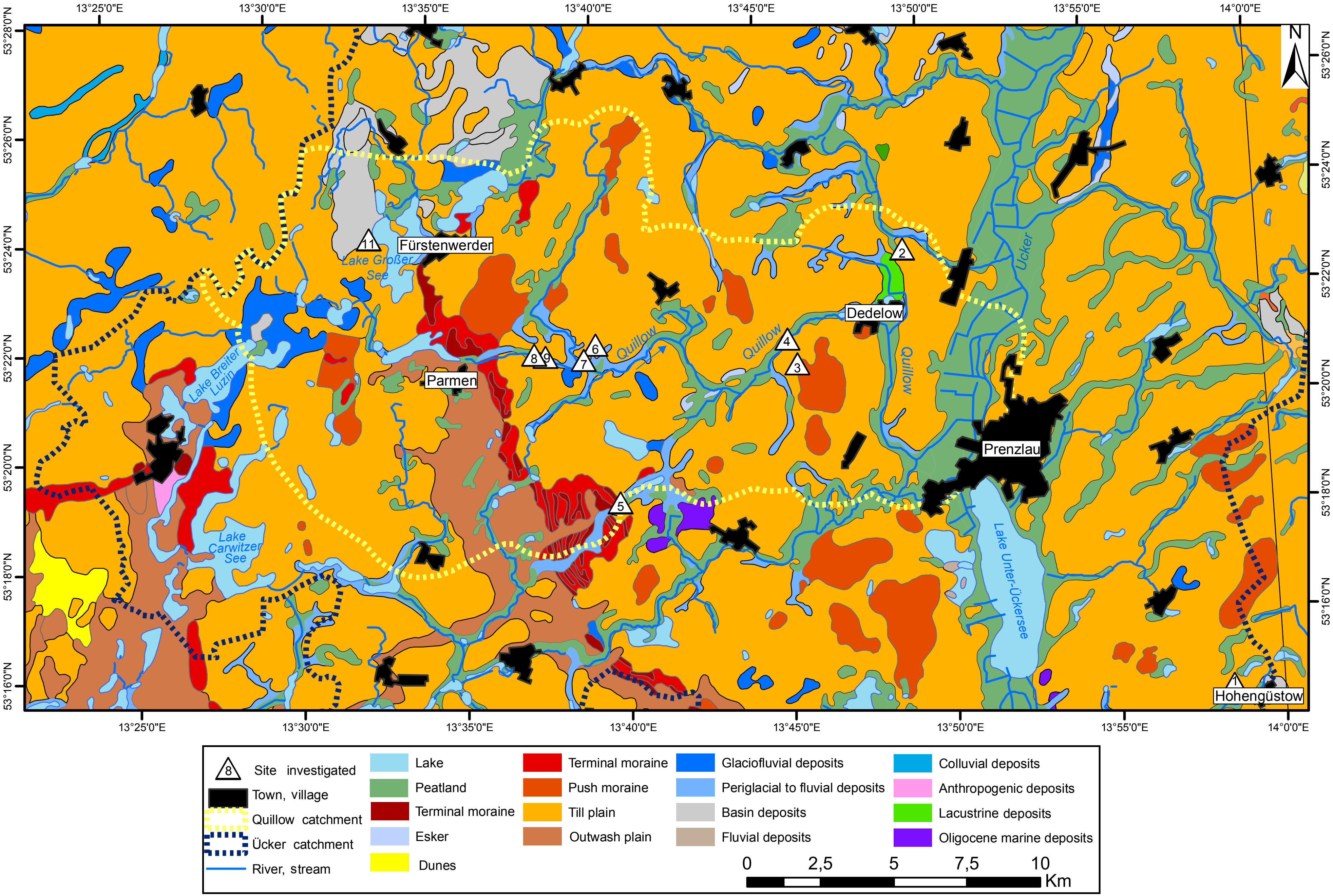

13°25'0"E
13°30'0"E
13°35'0"E
13°40'0"E
13°45'0"E
13°50'0"E
13°55'0"E
14°0'0"E
53°28'0"N
53°26'0"N
53°24'0"N
53°22'0"N
53°20'0"N
53°18'0"N
53°16'0"N
N
Fürstenwerder
Lake Großer See
Lake Breiter Luzin
Parmen
Quillow
Dedelow
Ucker
Prenzlau
Lake Carwitzer See
Lake Unter-Ückersee
Hohengüstow
1
2
3
4
5
6
7
8
9
11
Site investigated
Town, village
Quillow catchment
Ücker catchment
River, stream
Lake
Peatland
Terminal moraine
Esker
Dunes
Terminal moraine
Push moraine
Till plain
Outwash plain
Glaciofluvial deposits
Periglacial to fluvial deposits
Basin deposits
Fluvial deposits
Colluvial deposits
Anthropogenic deposits
Lacustrine deposits
Oligocene marine deposits
0
2,5
5
7,5
10
Km

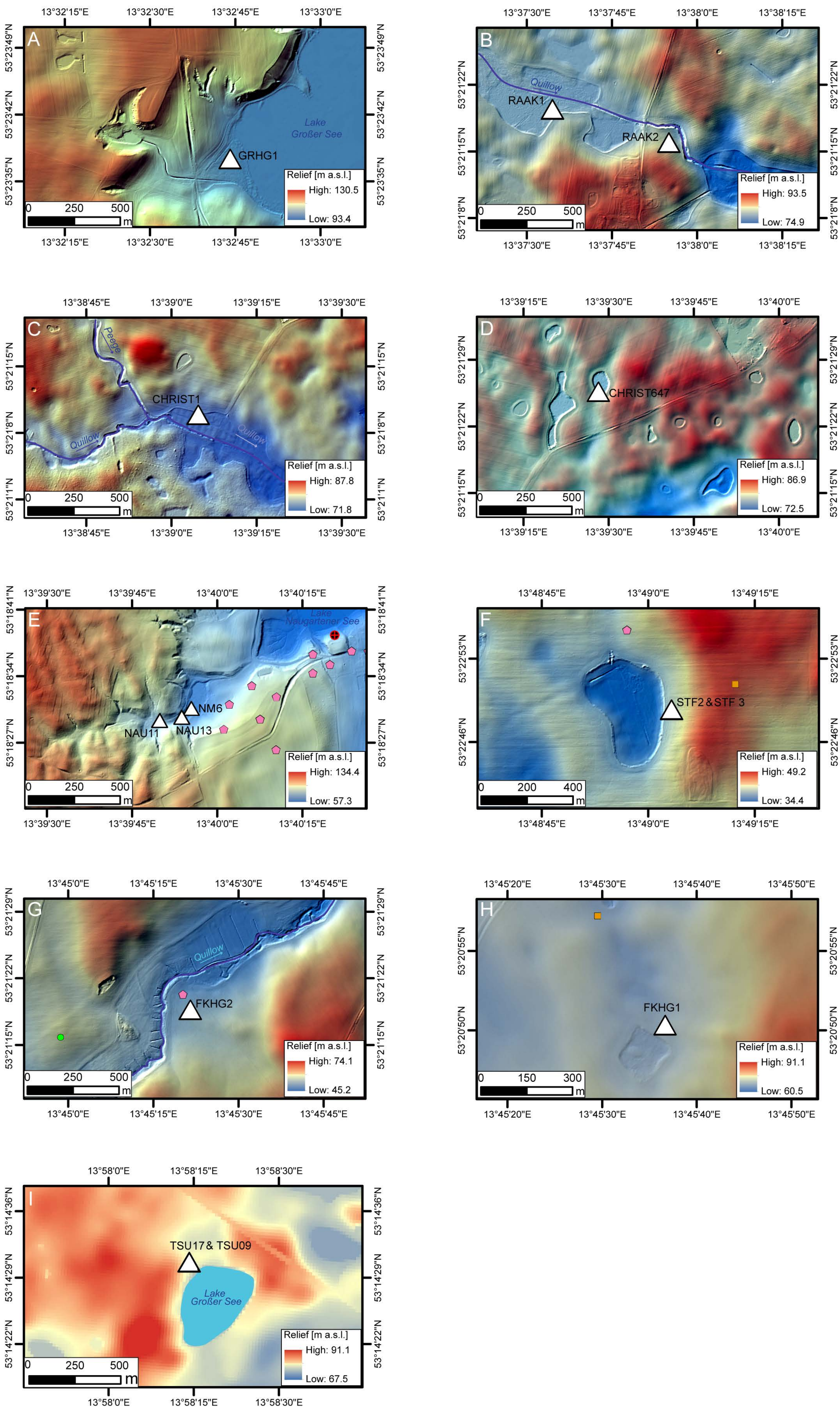

A
13°32'15"E
13°32'30"E
13°32'45"E
13°33'0"E
53°23'49"N
53°23'42"N
53°23'35"N
Lake
Großer See
GRHG1
Relief [m a.s.l.]
High: 130.5
Low: 93.4
0 250 500 m
B
13°37'30"E
13°37'45"E
13°38'0"E
13°38'15"E
53°21'22"N
53°21'15"N
53°21'8"N
Quillow
RAAK1
RAAK2
Relief [m a.s.l.]
High: 93.5
Low: 74.9
0 250 500 m
C
13°38'45"E
13°39'0"E
13°39'15"E
13°39'30"E
53°21'15"N
53°21'8"N
53°21'1"N
Peege
CHRIST1
Quillow
Quillow
Relief [m a.s.l.]
High: 87.8
Low: 71.8
0 250 500 m
D
13°39'15"E
13°39'30"E
13°39'45"E
13°40'0"E
53°21'29"N
53°21'22"N
53°21'15"N
CHRIST647
Relief [m a.s.l.]
High: 86.9
Low: 72.5
0 250 500 m
E
13°39'30"E
13°39'45"E
13°40'0"E
13°40'15"E
53°18'41"N
53°18'34"N
53°18'27"N
Lake
Naugartener See
NM6
NAU11
NAU13
Relief [m a.s.l.]
High: 134.4
Low: 57.3
0 250 500 m
F
13°48'45"E
13°49'0"E
13°49'15"E
53°22'53"N
53°22'46"N
STF2 & STF 3
Relief [m a.s.l.]
High: 49.2
Low: 34.4
0 200 400 m
G
13°45'0"E
13°45'15"E
13°45'30"E
13°45'45"E
53°21'29"N
53°21'22"N
53°21'15"N
Quillow
FKHG2
Relief [m a.s.l.]
High: 74.1
Low: 45.2
0 250 500 m
H
13°45'20"E
13°45'30"E
13°45'40"E
13°45'50"E
53°20'55"N
53°20'50"N
FKHG1
Relief [m a.s.l.]
High: 91.1
Low: 60.5
0 150 300 m
I
13°58'0"E
13°58'15"E
13°58'30"E
53°14'36"N
53°14'29"N
53°14'22"N
TSU17 & TSU09
Lake
Großer See
Relief [m a.s.l.]
High: 91.1
Low: 67.5
0 250 500 m

Supplement 3: De-Distributions of the obtained OSL ages:

CHRIST1-OSL 1 (HUB-558)

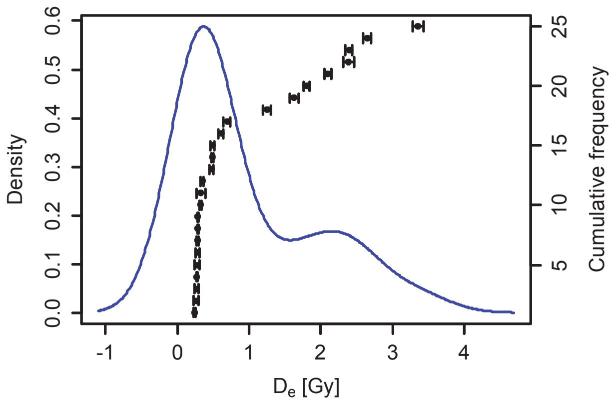

FKHG1 - OSL 1 (HUB-559)

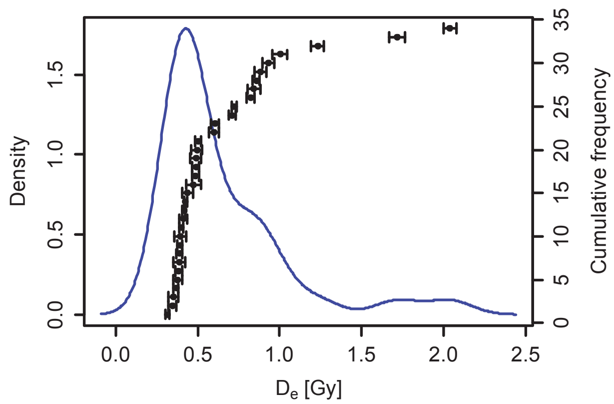

FKHG1 - OSL 2 (HUB-560)

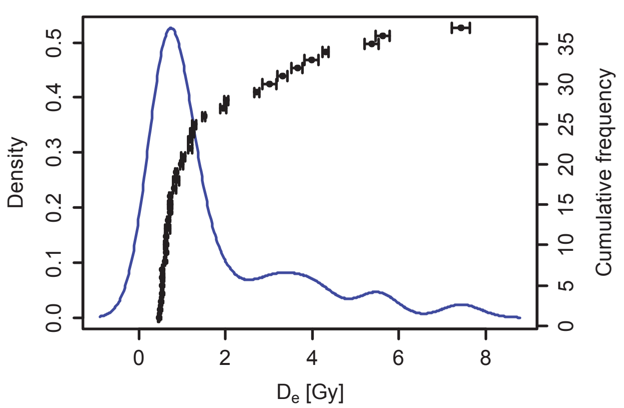

FKHG2 - OSL 2 (HUB-561)

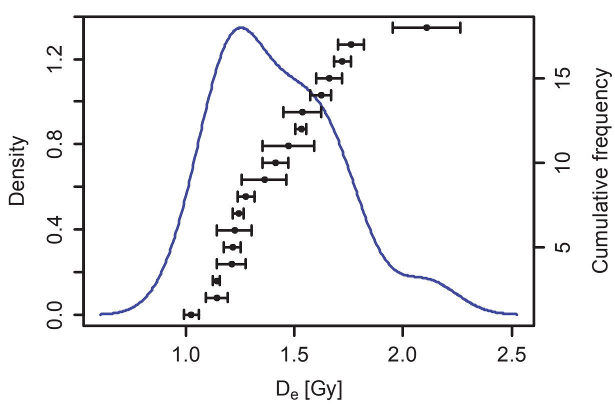

FKHG2 - OSL 3 (HUB-562)

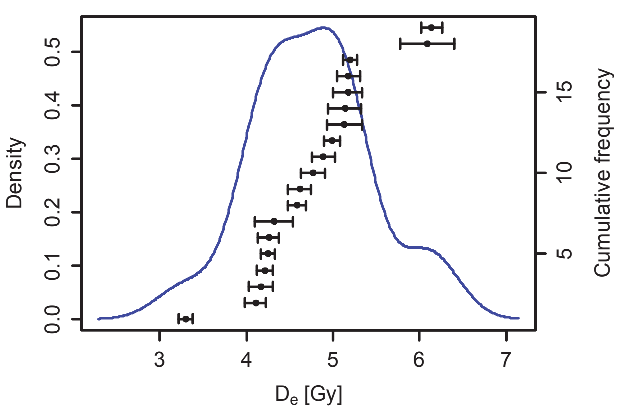

GRHG1 - OSL 1 (HUB-563)

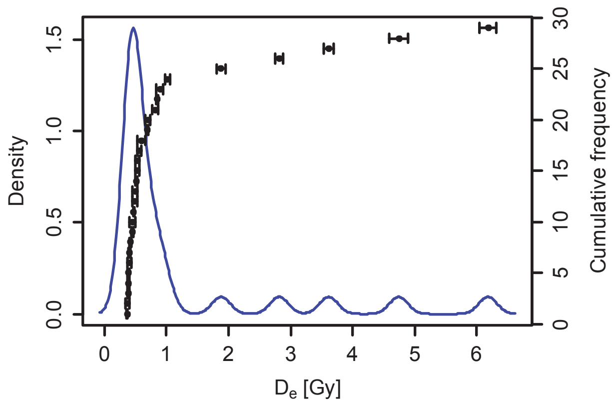

GRHG1 - OSL 2 (HUB-564)

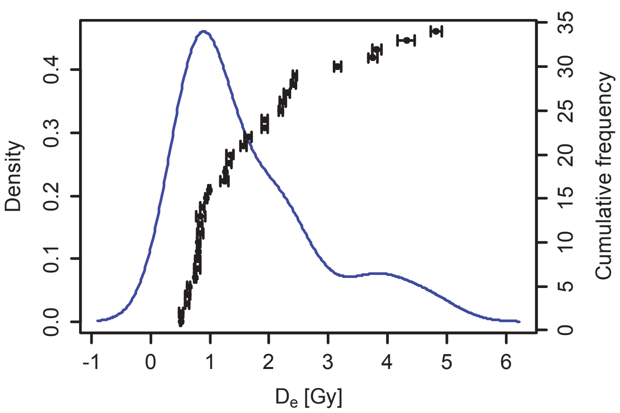

RAAK1 - OSL 1 (HUB-565)

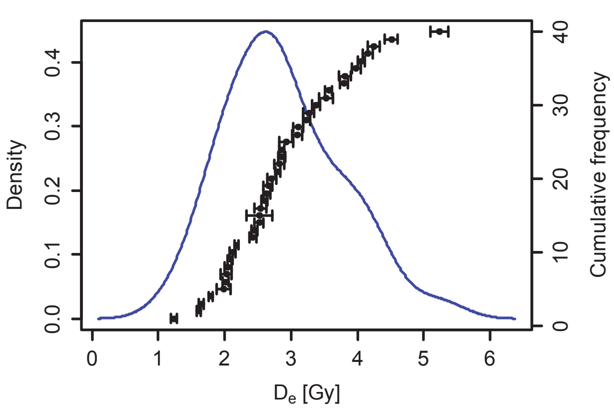

Supplement 3: De-Distributions of the obtained OSL ages:

RAAK1 - OSL 2 (HUB-566)

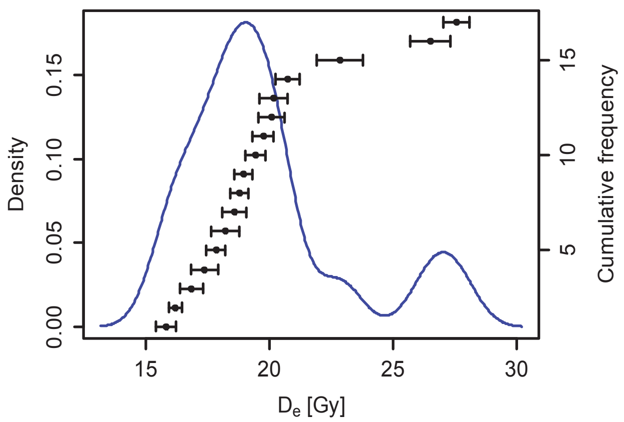

RAAK2 - OSL 3 (HUB-567)

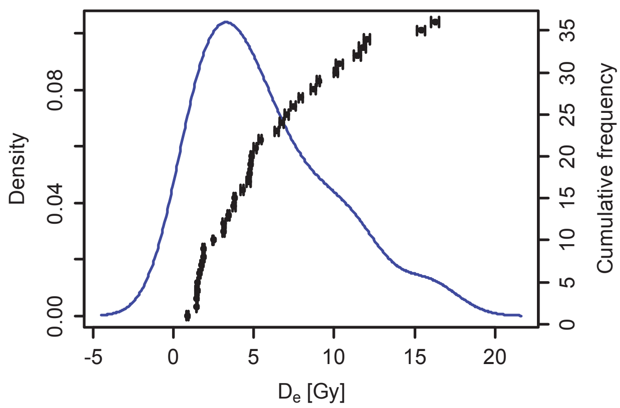

STFP2 - OSL 1 (HUB-568)

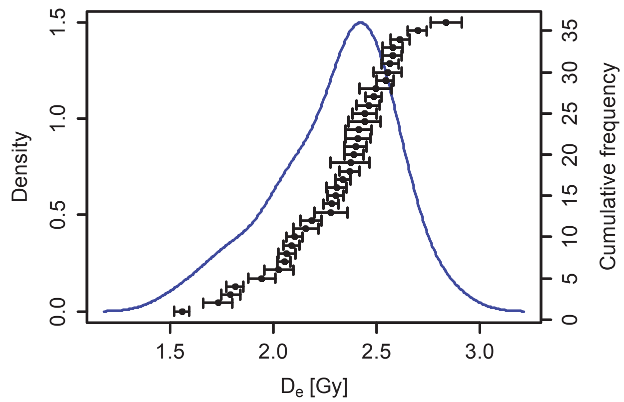

STFP2 - OSL 2 (HUB-569)

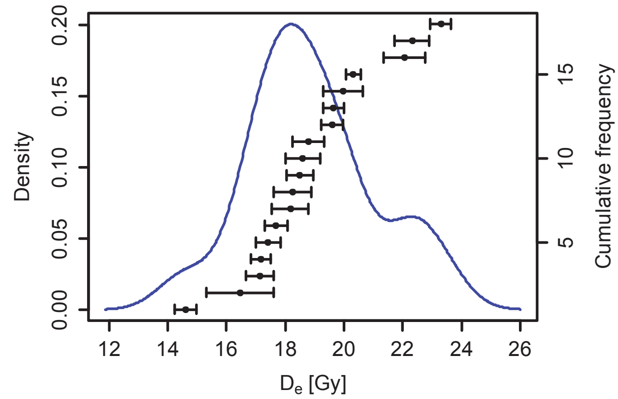

STFP2 - OSL 3 (HUB-570)

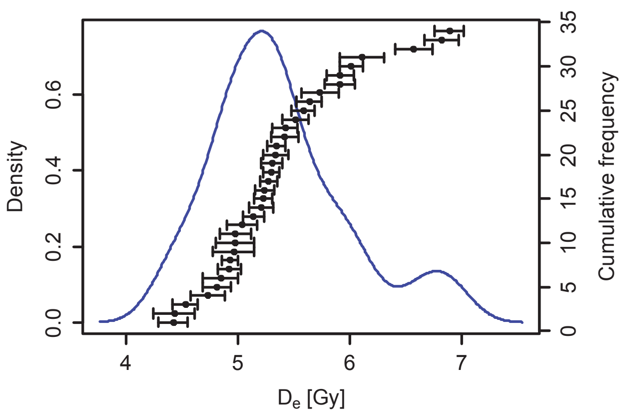

STFP3 - OSL 8 (HUB-571)

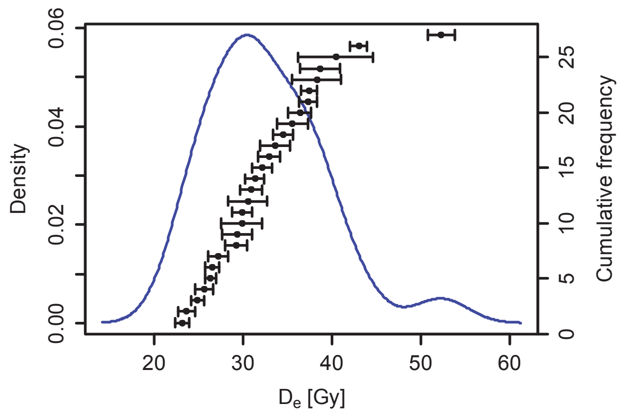

STFP3 - OSL 7 (HUB-572)

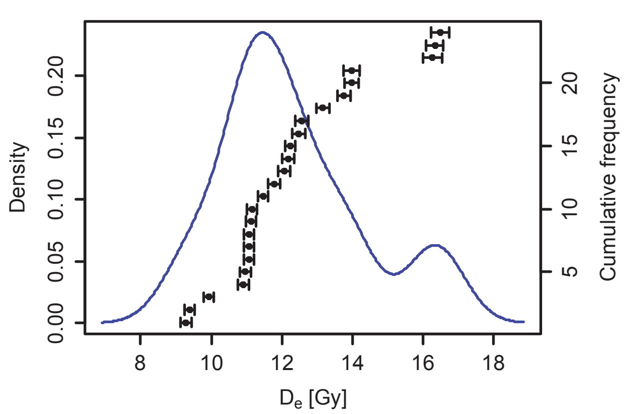

STFP3 - OSL 5 (HUB-573)

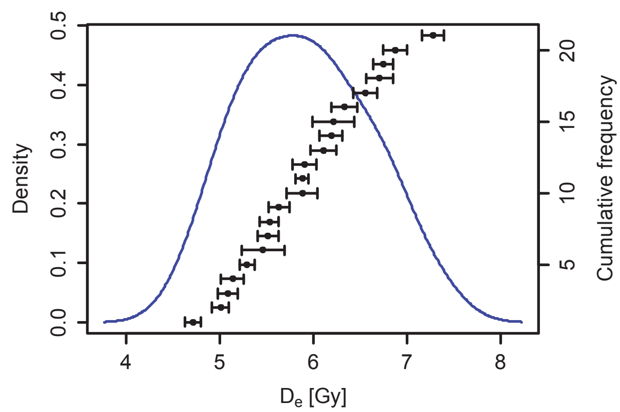

Supplement 3: De-Distributions of the obtained OSL ages:

STFP3 - OSL 4 (HUB-557)

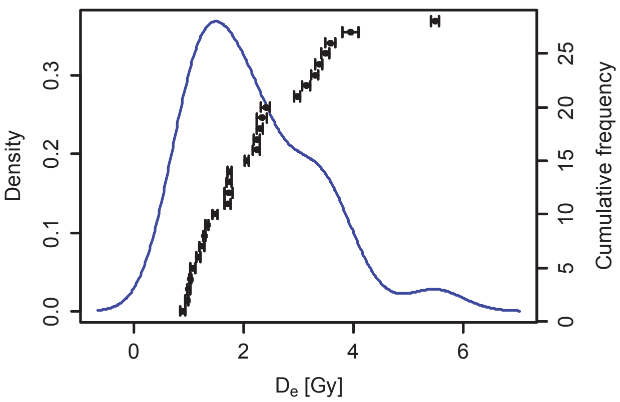

STFP3 - OSL 2 (HUB-575)

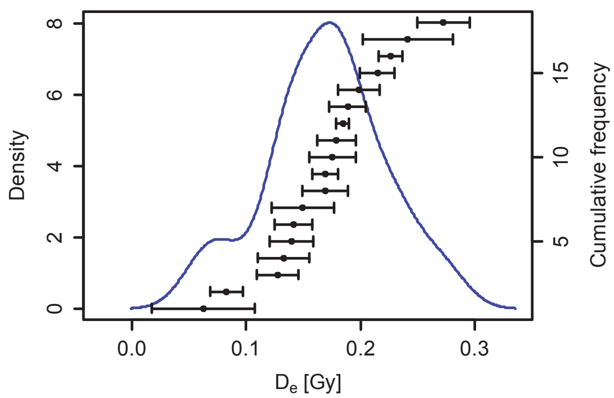

NAU13 - OSL2 (HUB-608)

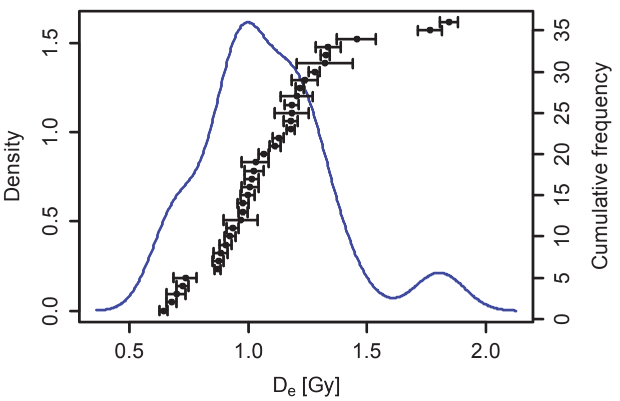

NM6 - OSL1 (HUB-609)

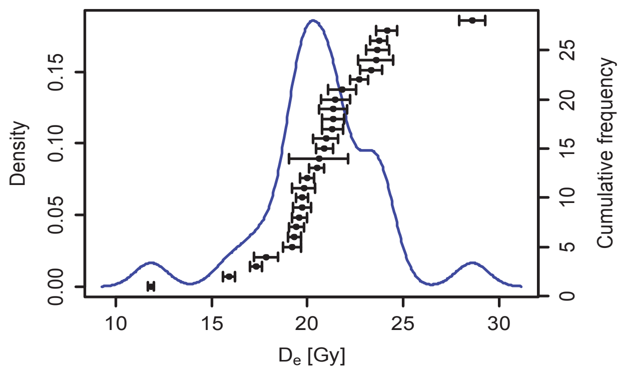

NM6 - OSL6 (HUB-610)

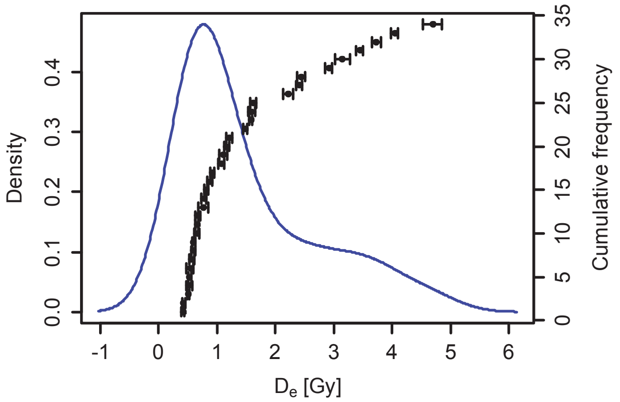

NAU13 - OSL3 (HUB-611)

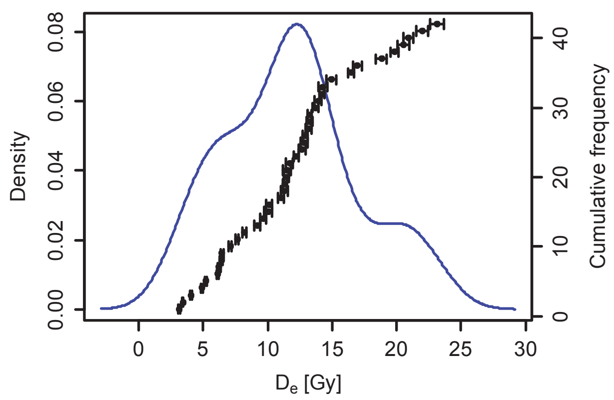

NAU13 - OSL1 (HUB-612)

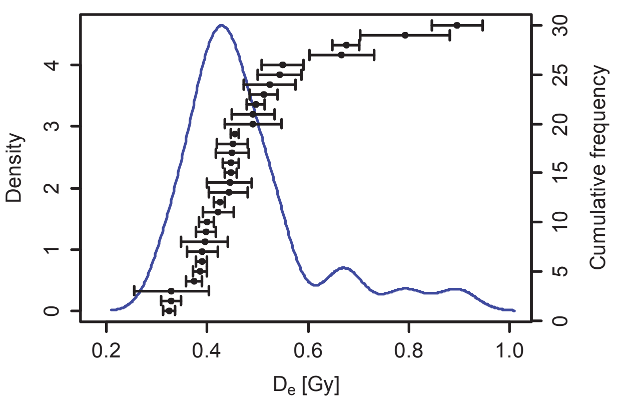

NAU11 - OSL3 (HUB-613)

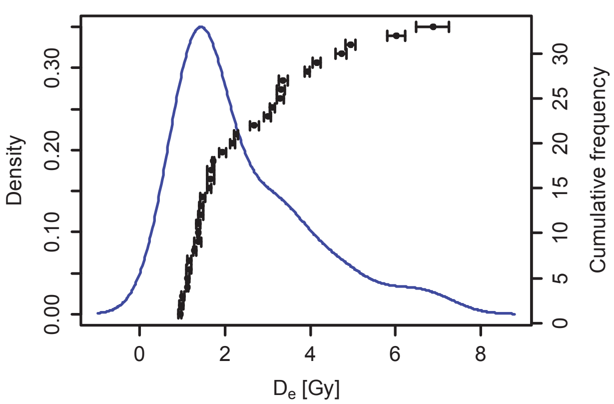

Supplement 3: De-Distributions of the obtained OSL ages:

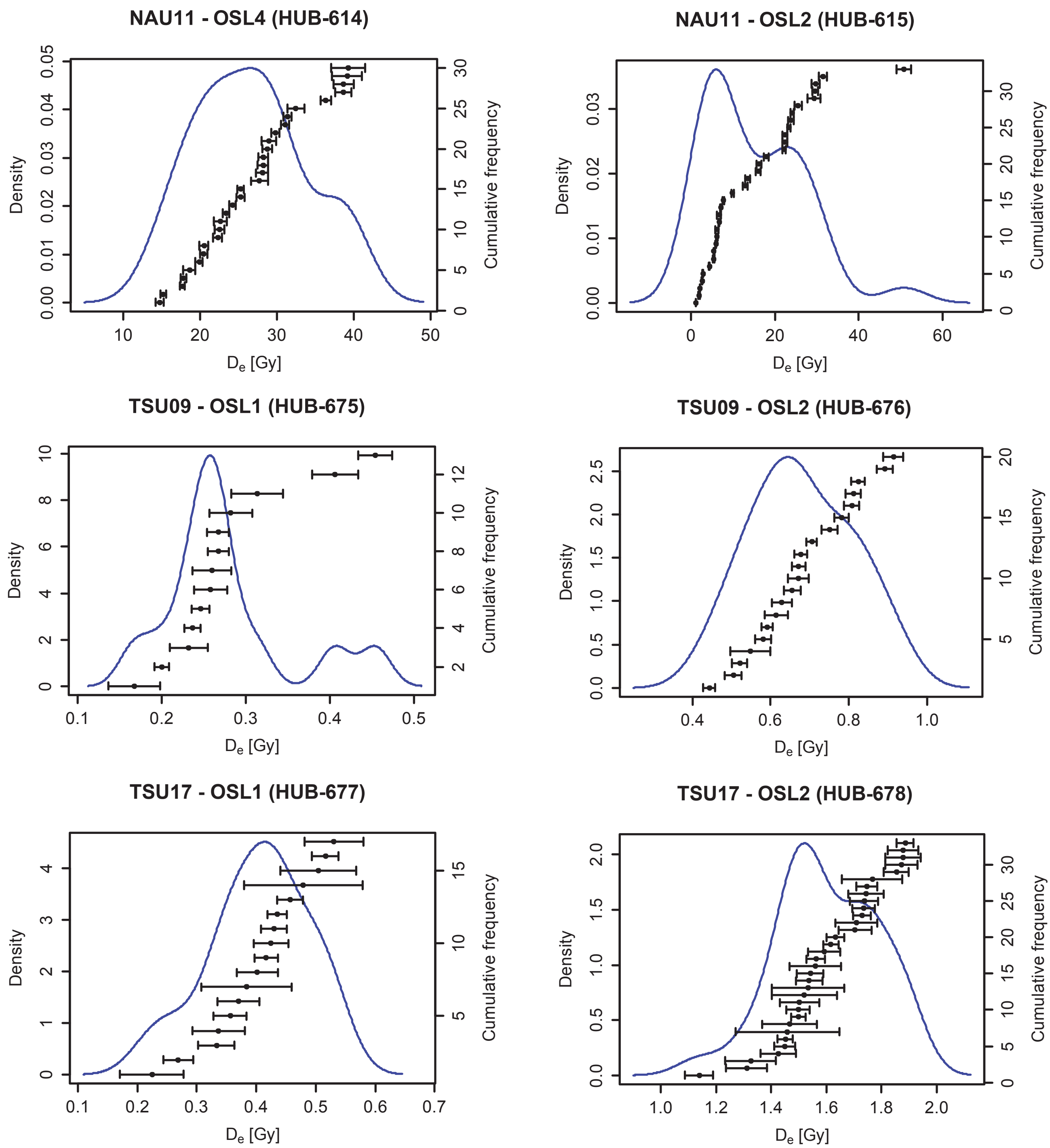

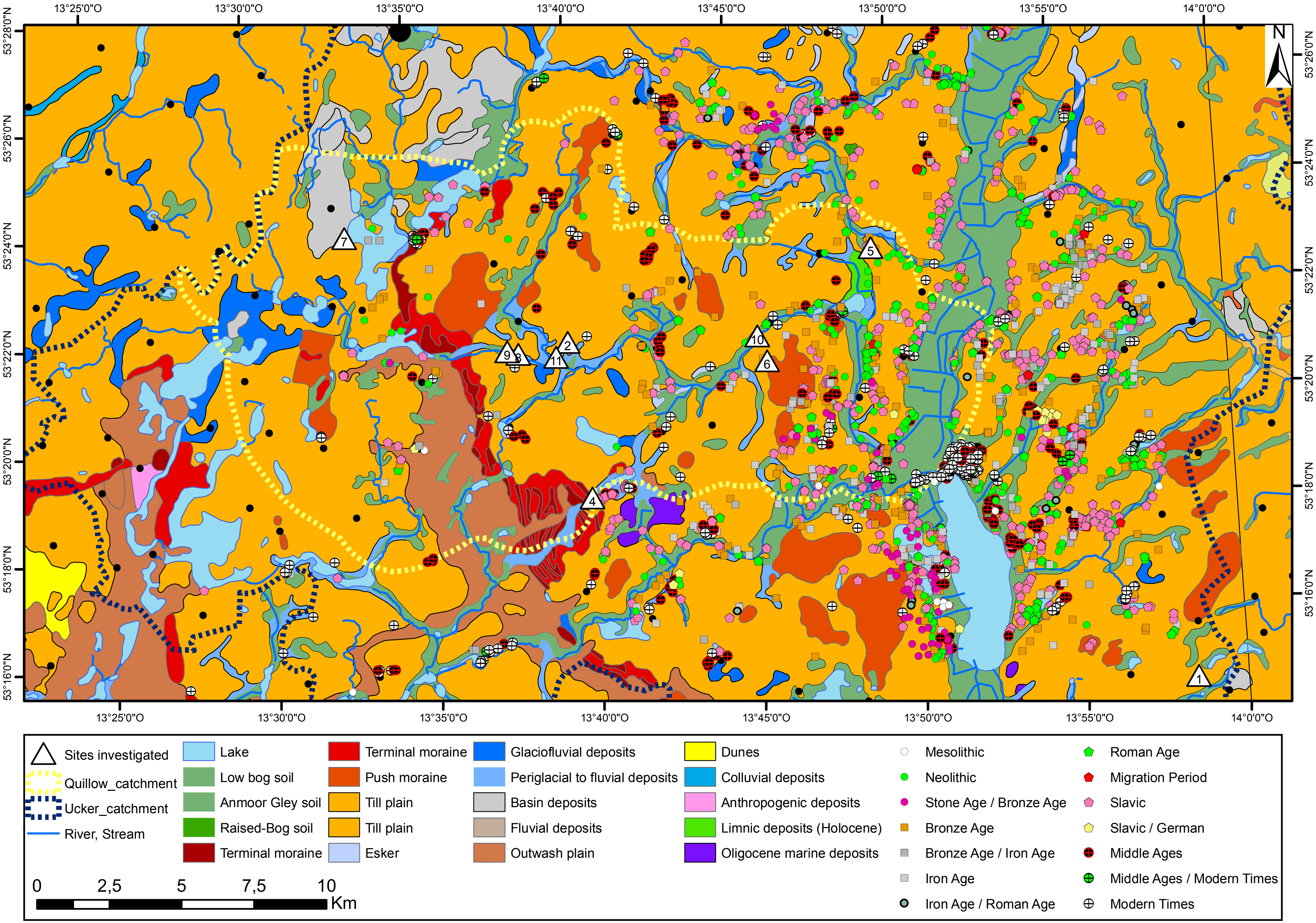
13°25'0"O
13°30'0"O
13°35'0"O
13°40'0"O
13°45'0"O
13°50'0"O
13°55'0"O
14°0'0"O
53°28'0"N
53°26'0"N
53°24'0"N
53°22'0"N
53°20'0"N
53°18'0"N
53°16'0"N
N
Sites investigated
Quillow_catchment
Ucker_catchment
River, Stream
Lake
Low bog soil
Anmoor Gley soil
Raised-Bog soil
Terminal moraine
Esker
Push moraine
Till plain
Glaciofluvial deposits
Periglacial to fluvial deposits
Basin deposits
Fluvial deposits
Outwash plain
Dunes
Colluvial deposits
Anthropogenic deposits
Limnic deposits (Holocene)
Oligocene marine deposits
Mesolithic
Neolithic
Stone Age / Bronze Age
Bronze Age
Bronze Age / Iron Age
Iron Age
Iron Age / Roman Age
Roman Age
Migration Period
Slavic
Slavic / German
Middle Ages
Middle Ages / Modern Times
Modern Times
0
2,5
5
7,5
10
Km

Profile	Horizon	Depth	% Clay <2µm	% Fine Silt 2-6.3µm
CHRIST1	Ah	0-15	3,17	4,76
CHRIST1	M	15-75	2,67	4,18
CHRIST1	M	15-75	9,72	13,66
CHRIST1	M	75-115	6,20	10,23
CHRIST1	M	75-115	8,37	11,97
CHRIST1	II fAxh	115-150	2,83	5,17
CHRIST1	II fAxh	115-150	4,63	5,79
CHRIST1	II Gr	150-175+	2,02	3,71
GRAUHG1	Ah	0-10	2,64	5,82
GRAUHG1	M	10-18	2,01	4,38
GRAUHG1	II M	18-40	4,14	5,95
GRAUHG1	II M	40-70	1,58	3,66
GRAUHG1	III M	70-80	1,56	2,59
GRAUHG1	III M	80-94	3,80	4,40
GRAUHG1	IV fAh	96-125	1,80	3,41
GRAUHG1	IV M	125-145	0,90	1,76
GRAUHG1	V fAh	145-173	4,52	6,96
GRAUHG1	V elGro	173-215	2,37	4,74
FKHG2	Ah	0-37	4,13	6,02
FKHG2	M	37-53	3,29	4,01
FKHG2	M	53-62	5,36	5,83
FKHG2	M	62-87	4,07	4,77
FKHG2	II fAh	87-96	8,66	9,42
FKHG2	II M	144-153	4,50	3,04
FKHG2	II M	144-153	16,36	4,45
FKHG2	II M	153-160	5,92	3,14
RAAK 1	Ah	0-9	2,61	4,24
RAAK 1	M	9-40	2,11	3,57
RAAK 1	M	40-70	1,69	3,65
RAAK 1	M-fAh	70-90	1,04	2,20
RAAK 1	M-fAh	90-113	2,99	5,65
RAAK 1	II fAh	113-120	0,35	1,34
RAAK 1	II Gr	120-150+	0,46	1,65
RAAK 2	Ah	0-5	4,29	7,68
RAAK 2	M	5-11	5,10	6,85
RAAK 2	M	11-72	5,72	8,65
RAAK 2	M	11-72	3,52	5,25
RAAK 2	II M	72-88	7,46	9,50
RAAK 2	II M	72-88	9,38	11,29
RAAK 2	III fAxh	88-128	10,19	11,87
RAAK 2	III elCc-rGr	128-150+	4,43	6,31
STF2	Ap	0-18	2,16	2,82
STF2	M	18-45	3,33	3,70
STF2	M	45-71	2,68	3,45

STF2	Sw-M	71-104	2,03	3,06
STF2	II fAh	104-110	3,17	4,57
STF2	II M	110-118	2,58	4,31
STF2	II M	111-118	1,69	3,77
STF2	III fAh	118-131	2,44	3,66
STF2	IV ilC	131-145	0,36	1,13
STF2	IV ilC	145-161	0,28	1,54
STF2	V ilC	161-181	0,24	2,07
STF2	V ilC	181-190	8,97	6,00
STF2	VI elC	190-230	6,84	6,11
STF3	Ap	0-20	3,14	3,54
STF3	M	20-130	2,96	3,68
STF3	M	20-130	3,01	3,65
STF3	M	20-130	2,08	3,01
STF3	M	20-130	2,80	3,68
STF3	Sw-M	130-145	9,82	15,84
STF3	II fHv	145-164	4,74	7,43
STF3	III ilC	164-173	0,35	0,63
STF3	III ilC	173-200	0,38	0,92
STF3	III ilC	200-206	0,58	1,84
STF3	III ilC	206-216	3,80	5,72
STF3	IV ilC	216-248	0,91	1,97
STF3	V fAxh	248-260	7,68	9,08
STF3	IV fAxh	260-275	5,83	7,94
STF3	VI elC	275-360	1,59	2,84
FKHG1	Ap	0-20	6,02	7,57
FKHG1	M	20-60	3,49	4,35
FKHG1	M	20-60	5,38	6,70
FKHG1	M	60-75	2,02	4,09
FKHG1	M	75-86	1,57	3,93
FKHG1	M	86-103	2,18	4,77
FKHG1	II fAh	103-110	6,00	7,82
FKHG1	II IlC	110-123	1,15	1,73
TSU09	Ah	0-15	4,92	7,51
TSU09	M	15-52	5,22	7,62
TSU09	II M	52-85	4,59	7,17
TSU09	II M	85-106	3,31	5,62
TSU09	II M	106-128	2,78	5,64
TSU09	III fAh	128-166	6,63	11,61
TSU09	III Gr	166 - 200	3,88	5,99
TSU17	Ah	0-30	5,19	6,07
TSU17	M	30-95	7,01	9,29
TSU17	M	95-130	5,35	8,60
TSU17	Gro	130-160	5,53	6,26
TSU17	Gro	160-190	4,19	6,80
TSU17	Gro	190-217	1,90	4,24

TSU17	II fAh	217-222	3,94	7,36
TSU17	II fAh	222-228	5,47	9,69
TSU17	II Gor	an 228	0,99	2,55
TSU17	II Gor	130-217	4,10	6,45
NAU11	Ah	0-3	-	-
NAU11	M	3-20	0,55	1,62
NAU11	II M	20-27	0,36	1,25
NAU11	II M	27-30	1,28	2,27
NAU11	III M	30-31	2,26	4,95
NAU11	III M	31-50	0,23	1,07
NAU11	III M	50-52	1,79	3,61
NAU11	III M	52-60	0,57	2,04
NAU11	III M	60-62	6,70	9,12
NAU11	III M	62-82	0,12	0,92
NAU11	III M	82-100	4,30	5,83
NAU11	IV fB(t)v	100-140	1,77	3,09
NAU11	V fAh	140-160	3,95	6,16
NAU11	V fAh	160-170	1,48	2,52
NAU11	V ilCv	170-200	0,49	1,63
NAU11	V ilCv	200-230	0,33	1,06
NAU11	V ilCv	200-230	1,05	1,23
NAU13	Ah	1-4	1,04	2,61
NAU13	A(e)h	5-8	0,97	2,40
NAU13	M	20-38	1,11	2,09
NAU13	II M	45-60	1,05	2,22
NAU13	II M	67-84	0,85	1,73
NAU13	III M	91-99	0,84	2,21
NAU13	IV M	102-131	0,94	2,08
NAU13	IV M	143-158	1,71	3,04
NAU13	V fojAh	161-177	0,22	1,58
NAU13	V fBv	182-193	2,80	3,44
NAU13	V fBv	202-214	2,79	4,01
NAU13	V fBv	216-228	4,40	5,92
NM6	M	4-5	0,69	2,19
NM6	M	9-11	0,58	1,64
NM6	M	22-25	0,00	0,12
NM6	M	40-42	0,49	1,52
NM6	M	50-53	2,95	5,85
NM6	M	60-64	8,29	12,49
NM6	II fH	72-74	-	-
NM6	II fH	90-92	-	-
NM6	II fH	96-97	-	-
NM6	III M	112-114	0,41	1,32
NM6	III M	139-142	0,00	0,25
NM6	IV fH	148-150	#	#
NM6	IV fH	152-153	#	#

NM6	V M	154-155	1,42	3,02
NM6	V M	167-172	0,55	1,62
NM6	V M	159-162	0,37	1,43
NM6	VI fH	195-197	#	#
NM6	VII M	220-230	0,10	0,58
NM6	VII M	260-270	0,00	0,00
NM6	VII M	310-315	0,33	0,84
NM6	VII M	319-320	0,11	0,77
NM6	VIII fH	317-319/320-322	-	-
NM6	IX M	328-330	0,13	1,02
NM6	X fH	340-350	-	-
NM6	X fH	340-350	-	-
NM6	XI Gr	378-380	1,03	2,63
NM6	XI Gr	390-405	0,37	1,09

% Middle Silt 6.3-20µm	% Coarse Silt 20-63µm	% Fine Sand 63-200µm	% Middle Sand 200-630µm	% Coarse Sand 630-2000µm	%Fine Gravel 2-2.5mm
8,61	7,50	25,29	42,24	8,43	0,00
7,24	5,82	25,88	45,17	9,04	0,00
27,86	14,04	13,50	19,38	1,84	0,00
15,02	8,39	15,41	38,17	6,60	0,00
15,59	9,58	15,38	36,32	2,80	0,00
9,92	13,71	23,41	38,43	6,54	0,00
12,57	10,04	15,28	35,92	15,76	0,00
9,95	26,18	23,29	28,70	6,15	0,00
9,93	11,60	32,71	36,80	0,52	0,00
8,00	10,27	35,48	38,76	1,11	0,00
10,68	10,72	27,91	37,39	3,22	0,00
6,79	10,05	35,47	39,08	3,37	0,00
4,60	4,94	28,40	45,67	12,06	0,18
7,17	9,51	36,17	36,71	2,24	0,00
6,85	8,18	29,87	43,80	6,09	0,00
2,81	6,85	41,60	41,73	4,35	0,00
11,24	6,98	24,16	39,01	7,12	0,00
8,18	5,91	22,79	41,59	14,43	0,00
8,53	7,28	20,80	32,41	20,83	0,00
6,88	5,70	25,48	41,87	12,78	0,00
7,36	8,82	32,10	35,32	5,22	0,00
7,59	6,66	29,89	39,43	7,60	0,00
17,50	15,81	35,29	13,32	0,00	0,00
5,44	4,76	22,52	45,15	14,58	0,00
3,30	6,21	42,01	27,63	0,04	0,00
6,11	5,58	25,63	44,14	9,49	0,00
7,21	4,71	22,15	46,61	12,47	0,00
5,92	3,94	20,09	52,46	11,92	0,00
5,90	6,00	36,95	40,91	4,90	0,00
3,35	3,29	24,76	49,88	14,58	0,92
9,12	11,58	29,96	37,93	2,76	0,00
2,19	3,06	23,34	45,28	24,45	0,00
2,71	3,97	30,85	51,14	9,22	0,00
10,66	10,25	24,20	36,34	6,59	0,00
10,41	6,26	23,88	40,74	6,77	0,00
12,21	12,62	26,27	33,39	1,15	0,00
8,83	5,56	22,00	43,24	11,61	0,00
11,53	9,06	19,71	36,27	6,47	0,00
18,94	11,70	30,92	17,77	0,00	0,00
24,06	12,73	23,91	17,21	0,04	0,00
11,80	5,18	23,85	39,49	8,94	0,00
4,57	4,42	21,75	48,66	15,38	0,24
6,20	5,52	26,16	41,86	13,24	0,00
5,82	6,29	22,79	42,03	16,52	0,42

5,14	4,92	17,39	50,25	17,21	0,00
8,53	5,33	17,35	44,32	16,73	0,00
7,65	6,11	18,11	39,15	21,44	0,64
6,05	5,67	20,42	49,90	12,51	0,00
6,73	5,55	20,88	43,98	16,77	0,00
1,73	4,25	25,56	47,69	19,28	0,00
2,64	3,21	26,67	46,66	19,00	0,00
3,74	6,57	61,35	26,03	0,00	0,00
9,35	12,38	54,40	8,90	0,00	0,00
14,53	15,77	26,17	23,51	7,07	0,00
6,39	4,90	17,36	39,51	22,95	2,22
6,33	5,86	24,12	36,78	19,26	1,02
6,04	5,87	25,31	42,87	13,26	0,00
4,93	5,27	25,28	39,98	18,86	0,59
6,38	5,35	18,47	40,25	22,50	0,59
33,34	20,93	17,27	2,79	0,00	0,00
15,44	14,19	20,60	33,26	4,34	0,00
1,19	3,99	40,80	43,74	9,30	0,00
1,37	4,93	48,16	39,84	4,40	0,00
2,06	7,87	57,63	28,98	1,05	0,00
8,97	9,73	42,48	28,69	0,61	0,00
3,15	5,46	37,15	40,66	9,88	0,82
18,83	14,12	28,02	20,57	1,71	0,00
17,30	19,40	27,48	20,32	1,74	0,00
7,58	14,86	24,11	38,57	10,44	0,00
10,40	10,06	32,51	27,75	5,69	0,00
6,85	7,77	34,38	37,06	6,09	0,00
12,64	14,27	50,08	10,94	0,00	0,00
6,12	9,68	43,11	30,60	4,39	0,00
6,40	12,26	46,37	27,67	1,81	0,00
7,88	9,58	37,88	33,82	3,90	0,00
10,36	11,51	33,65	26,65	4,01	0,00
2,52	4,73	36,97	42,38	10,52	0,00
12,65	11,57	19,15	38,79	5,41	-
11,25	11,34	20,22	38,50	5,86	-
10,64	11,75	22,17	39,97	3,73	-
10,27	8,17	20,11	37,83	14,70	-
10,26	7,80	20,57	43,12	9,83	-
20,80	13,72	21,97	21,53	3,74	-
10,82	9,24	23,46	37,28	9,34	-
12,30	7,79	20,74	40,69	7,23	-
13,16	12,60	21,31	32,90	3,73	-
13,43	13,23	18,83	40,26	0,30	-
11,61	8,08	19,23	34,94	14,26	-
11,01	11,83	22,52	36,93	6,71	-
7,61	6,92	21,58	43,96	13,78	-

12,22	10,32	21,20	40,44	4,54	-
19,30	14,89	28,51	20,91	1,23	-
4,55	6,53	32,88	44,36	8,15	-
11,69	11,27	21,70	38,25	6,55	-
-	-	-	-	-	-
2,71	2,19	7,39	53,92	31,62	5,87
1,63	1,46	10,71	63,57	21,03	3,68
3,78	2,76	7,83	39,53	42,55	15,79
13,16	13,19	10,92	33,23	22,31	1,22
1,28	0,18	9,17	73,35	14,74	3,01
7,08	18,05	33,94	35,02	0,52	0,00
2,48	5,89	49,42	39,51	0,10	0,00
19,45	16,36	24,25	23,62	0,49	0,00
0,80	0,02	11,32	73,17	13,65	2,48
11,43	8,54	12,96	47,53	9,41	0,00
5,02	2,63	11,21	58,47	17,83	2,24
10,69	5,10	14,57	55,10	4,43	5,29
3,82	2,59	14,86	63,88	10,84	5,59
2,84	3,19	20,76	62,97	8,12	21,14
1,27	1,78	27,07	64,99	3,50	1,29
1,64	1,70	24,23	65,44	4,71	4,71
4,47	3,26	15,37	61,83	11,42	1,81
4,05	3,46	14,48	62,05	12,57	3,55
3,90	3,24	13,38	59,56	16,73	8,02
4,23	3,56	16,44	64,26	8,24	3,42
3,06	2,58	10,85	61,20	19,75	5,44
3,83	3,13	11,98	62,43	15,58	3,02
3,10	3,19	15,80	64,70	10,21	3,71
5,45	4,20	12,15	63,49	9,93	2,93
3,65	3,56	10,51	68,71	11,76	8,97
6,11	3,66	9,17	58,35	16,51	10,49
7,12	3,86	7,88	50,33	24,01	13,04
9,84	6,29	11,09	51,37	11,12	2,71
5,11	6,20	14,26	57,52	14,02	9,38
2,65	2,57	12,26	60,74	19,57	4,12
0,56	0,11	6,17	71,69	21,35	2,63
2,01	1,57	25,97	66,82	1,62	1,19
9,69	17,51	54,91	9,08	0,00	0,00
27,33	19,12	16,86	13,93	1,96	2,58
-	-	-	-	-	-
-	-	-	-	-	-
-	-	-	-	-	-
1,58	1,07	14,41	75,08	6,14	0,00
0,46	0,00	5,85	81,22	12,22	1,33
#	#	#	#	#	#
#	#	#	#	#	#

4,03	8,83	40,85	40,71	1,15	0,00
1,55	2,83	47,30	45,90	0,24	0,00
2,24	1,11	3,69	44,67	46,50	17,62
#	#	#	#	#	#
0,63	0,56	13,42	71,67	13,06	8,94
0,33	0,00	2,55	62,52	34,60	8,40
1,09	2,71	24,08	63,42	7,52	5,15
1,18	1,91	13,93	60,88	21,22	31,33
-	-	-	-	-	-
1,39	0,25	2,86	61,82	32,53	17,44
-	-	-	-	-	-
-	-	-	-	-	-
5,76	6,07	16,05	58,31	10,13	2,79
1,32	2,13	20,23	59,04	15,84	0,63

% Corg	% $CaCO_3$
0,91	0,00
0,79	0,00
0,95	0,00
1,58	1,40
3,92	0,40
1,08	-0,20
0,79	0,40
-	-
2,44	0,00
0,82	0,00
1,32	0,00
0,50	0,00
0,31	0,00
0,21	0,00
0,46	0,00
0,25	0,00
1,10	0,00
0,19	0,00
0,82	0,00
0,62	0,00
0,32	0,00
0,34	0,00
0,58	1,13
0,36	0,00
0,36	0,00
0,78	0,50
2,08	0,00
1,14	0,50
0,56	0,00
0,46	0,40
1,21	0,00
0,17	0,00
0,06	0,00
1,31	0,00
0,76	0,00
0,81	0,80
0,81	0,80
1,12	0,80
1,12	0,80
3,69	0,10
0,17	13,30
0,77	0,20
0,66	0,00
0,31	0,00

0,29	0,00
1,71	0,00
0,32	7,36
0,95	0,00
1,35	0,00
0,13	4,79
?	?
0,84	0,00
0,15	0,00
0,07	0,00
0,14	0,00
0,86	0,00
1,13	0,10
0,54	0,00
0,73	0,00
2,84	0,25
7,33	0,52
0,61	0,00
0,19	0,00
0,28	0,00
0,52	0,00
0,24	0,00
1,82	0,00
0,82	0,00
0,64	0,00
0,51	0,00
0,12	0,14
1,28	0,76
0,55	2,12
0,54	2,61
0,39	0,77
0,64	2,04
0,24	0,17
2,23	-
-	-
0,89	-
0,46	-
0,64	-
2,67	-
0,46	-
1,55	-
0,46	-
-	-
-	-
-	-
0,31	-

0,98	-
2,33	-
-	-
-	-
-	-
1,06	0,16
0,57	0,15
0,77	0,25
1,98	0,50
0,31	0,13
1,91	0,42
0,59	0,21
2,58	0,67
0,28	0,14
2,19	0,62
1,25	0,32
3,19	0,44
0,75	0,22
0,39	0,18
0,20	0,13
0,88	0,36
3,02	0,23
2,23	0,22
1,02	0,25
1,10	0,27
0,70	0,21
0,98	0,21
0,57	0,17
3,14	0,46
8,52	1,28
2,89	0,47
3,46	0,60
4,00	0,76
15,24	0,50
3,29	0,22
0,35	0,13
0,77	0,18
2,84	0,41
8,48	0,95
74,15	7,41
93,95	20,11
93,01	25,03
0,51	0,68
0,21	1,03
75,54	6,05
85,48	10,46

1,21	1,00
0,40	0,86
0,28	1,64
93,07	21,82
0,27	0,78
0,25	1,30
0,52	0,77
-	-
21,13	1,64
0,36	1,42
47,89	2,44
-	-
2,32	0,25
0,41	0,14

Sample ID	Lab ID	Geogr. Pos.		Elevation asl	Sample depth	Grain size	U-238	Th-232	K-40	Cosm. DR	H2O	D_0	De (*)			OSL Age	
													CAM	OD	MAM (**)	CAM	MAM
		Latitude	Longitude	[m]	[cm]	[µm]	[Bq/kg]	[Bq/kg]	[Bq/kg]	[Gy/ka]	[Gew.-%]	[Gy/ka]	[Gy]	[%]	[Gy]	[ka]	[ka]
Christ1 - OSL 1	HUB-558	53,35196666	13,64643335	81	94	90 - 200	19.94 ± 1.6	20.65 ± 0.95	417.01 ± 10.5	0.18 ± 0.02	18.9 ± 5	1.85 ± 0.13	0.62 ± 0.11	89,3	0.3 ± 0.03	0.335 ± 0.064	0.162 ± 0.02
Fkhg1 - OSL 1	HUB-559	53,34685952	13,76050423	68	116	90 - 200	15.44 ± 2.27	18.5 ± 1.17	460.39 ± 9.9	0.18 ± 0.02	16.1 ± 5	1.94 ± 0.15	0.6 ± 0.05	46	0.42 ± 0.04	0.309 ± 0.035	0.216 ± 0.027
Fkhg1 - OSL 2	HUB-560	53,34685952	13,76050423	68	139	90 - 200	9.29 ± 0.52	9.18 ± 0.76	375.46 ± 9.16	0.18 ± 0.02	3.9 ± 3	1.62 ± 0.09	1.19 ± 0.16	80,6	0.61 ± 0.05	0.734 ± 0.107	0.377 ± 0.038
Fkhg2 - OSL 2	HUB-561	53,35436237	13,75499769	52	92	90 - 200	16.72 ± 1.13	18.56 ± 1.9	458.45 ± 10.09	0.18 ± 0.02	10.5 ± 4	2.06 ± 0.14	1.4 ± 0.06	15,9	-	0.68 ± 0.055	-
Fkhg2 - OSL 3	HUB-562	53,35436237	13,75499769	52	136	90 - 200	16.25 ± 1.3	21.53 ± 1.25	425.43 ± 9.4	0.18 ± 0.02	13 ± 5	1.91 ± 0.14	4.7 ± 0.15	12,9	-	2.466 ± 0.194	-
Grauh1 - OSL 1	HUB-563	53,39318082	13,5445372	96	90	90 - 200	11.64 ± 1.05	13.44 ± 0.95	429.85 ± 9.71	0.19 ± 0.02	1.3 ± 3	1.9 ± 0.11	0.73 ± 0.11	79,3	0.46 ± 0.03	0.384 ± 0.062	0.242 ± 0.021
Grauh1 - OSL 2	HUB-564	53,39318082	13,5445372	96	138	90 - 200	14.15 ± 1.25	14.56 ± 1.24	365.1 ± 8.54	0.18 ± 0.02	7.9 ± 4	1.68 ± 0.12	1.34 ± 0.15	63,4	0.71 ± 0.09	0.796 ± 0.105	0.422 ± 0.061
Raak1 - OSL 1	HUB-565	53,35666516	13,61792287	82	61	90 - 200	13.12 ± 1.51	15.98 ± 1.25	408.27 ± 9.22	0.19 ± 0.02	8.5 ± 4	1.82 ± 0.13	2.75 ± 0.13	30,5	2.06 ± 0.2	1.512 ± 0.129	1.133 ± 0.136
Raak1 - OSL 2	HUB-566	53,35666516	13,61792287	82	123	90 - 200	10.08 ± 0.88	9.9 ± 0.75	368.77 ± 8.59	0.18 ± 0.02	14.8 ± 5	1.48 ± 0.11	19.5 ± 0.7	13,9	-	13.171 ± 1.06	-
Raak2 - OSL 3	HUB-567	53,35451506	13,63261217	82	84	90 - 200	22.72 ± 2.62	26.33 ± 0.97	466.65 ± 10.53	0.19 ± 0.02	8.9 ± 4	2.31 ± 0.16	4.41 ± 0.57	76,6	1.42 ± 0.2	1.909 ± 0.281	0.615 ± 0.097
Steinfurth_P2 - OSL 1	HUB-568	53,3793735	13,81710991	35	88	90 - 200	14.91 ± 1.19	17.97 ± 1.07	429.96 ± 9.68	0.18 ± 0.02	4.2 ± 3	2.04 ± 0.12	2.29 ± 0.05	11,9	-	1.124 ± 0.071	-
Steinfurth_P2 - OSL 2	HUB-569	53,3793735	13,81710991	35	157	90 - 200	11.99 ± 0.95	11.42 ± 1.14	390.35 ± 9	0.18 ± 0.02	5.3 ± 3	1.75 ± 0.11	18.88 ± 0.51	10,1	-	10.793 ± 0.729	-
Steinfurth_P2 - OSL 3	HUB-570	53,3793735	13,81710991	35	137	90 - 200	10.48 ± 0.97	12.73 ± 1.17	378.59 ± 8.23	0.18 ± 0.02	1.6 ± 3	1.71 ± 0.11	5.36 ± 0.1	9,3	-	3.135 ± 0.205	-
Steinfurth_P3 - OSL 8	HUB-571	53,3793735	13,81710991	35	276	90 - 200	21.84 ± 1.18	23.93 ± 2.3	485.32 ± 11.05	0.16 ± 0.02	12.5 ± 5	2.18 ± 0.16	31.92 ± 1.22	17,9	-	14.66 ± 1.22	-
Steinfurth_P3 - OSL 7	HUB-572	53,3793735	13,81710991	35	252	90 - 200	17.96 ± 2.67	23 ± 0.58	430.82 ± 9.57	0.16 ± 0.02	17.2 ± 5	1.96 ± 0.15	12.12 ± 0.38	15,2	-	6.195 ± 0.52	-
Steinfurth_P3 - OSL 5	HUB-573	53,3793735	13,81710991	35	195	90 - 200	9.69 ± 0.61	9.38 ± 0.77	364.02 ± 8.32	0.17 ± 0.02	3.6 ± 3	1.59 ± 0.09	5.87 ± 0.15	10,8	-	3.693 ± 0.233	-
Steinfurth_P3 - OSL 4	HUB-574	53,3793735	13,81710991	35	134	90 - 200	19.11 ± 1.92	22.67 ± 1.63	478.09 ± 10.47	0.18 ± 0.02	15.1 ± 5	2.11 ± 0.16	1.94 ± 0.18	48,4	1.11 ± 0.14	0.919 ± 0.11	0.526 ± 0.077
Steinfurth_P3 - OSL 2	HUB-575	53,3793735	13,81710991	35	85	90 - 200	16.17 ± 1.25	19.01 ± 1.79	482.09 ± 10.97	0.18 ± 0.02	6.3 ± 3	2.32 ± 0.16	0.19 ± 0.01	7,1	-	0.082 ± 0.007	-
Nau13-OSL1	HUB-612	53,308144	13,664629	73	57	90 - 200	13.05 ± 0.56	14.56 ± 1.25	335.96 ± 7.52	0.19 ± 0.02	2.8 ± 3	1.67 ± 0.1	0.46 ± 0.02	19,3	-	0.28 ± 0.02	-
Nau13-OSL2	HUB-608	53,308144	13,664629	73	130	90 - 200	11.73 ± 1.04	12.99 ± 1.29	317.72 ± 7.33	0.18 ± 0.02	2.2 ± 3	1.56 ± 0.1	1.05 ± 0.04	22,9	1 ± 0.09	0.67 ± 0.05	0.64 ± 0.07
Nau13-OSL3	HUB-611	53,308144	13,664629	73	220	90 - 250	25.97 ± 6.54	55.21 ± 7.1	310.92 ± 7.11	0.17 ± 0.02	11.4 ± 4	2.34 ± 0.3	10.59 ± 0.8	49,1	4.89 ± 0.56	4.53 ± 0.67	2.09 ± 0.36
NM6-OSL6	HUB-610	53,308302	13,665362	69	42	90 - 200	21.53 ± 2.48	24.75 ± 1.23	465.9 ± 10.14	0.19 ± 0.02	20.1 ± 5	2.07 ± 0.16	1.15 ± 0.14	70,7	0.57 ± 0.08	0.56 ± 0.08	0.28 ± 0.04
NM6-OSL1	HUB-609	53,308302	13,665362	69	390	90 - 200	9.76 ± 1.4	12.78 ± 0.82	321.71 ± 7.39	0.15 ± 0.02	17.3 ± 5	1.3 ± 0.1	20.41 ± 0.63	15,4	-	15.66 ± 1.29	-
Nau11-OSL2	HUB-615	53,308054	13,663894	77	72	90 - 200	10.61 ± 1.73	11.44 ± 0.61	319.12 ± 7.53	0.19 ± 0.02	0.4 ± 3	1.52 ± 0.11	10.42 ± 1.69	93,1	1.81 ± 0.33	6.84 ± 1.21	1.19 ± 0.23
Nau11-OSL3	HUB-613	53,308054	13,663894	77	120	90 - 200	13.53 ± 1.64	14.59 ± 0.94	336.71 ± 7.8	0.18 ± 0.02	1.7 ± 3	1.68 ± 0.11	2.05 ± 0.2	55,4	1.27 ± 0.14	1.22 ± 0.15	0.76 ± 0.1
Nau11-OSL4	HUB-614	53,308054	13,663894	77	185	90 - 200	12.38 ± 1.02	14.67 ± 1.08	340.06 ± 7.61	0.17 ± 0.02	0.6 ± 3	1.66 ± 0.1	25.53 ± 1.25	26,2	20.86 ± 2.22	15.4 ± 1.22	12.59 ± 1.55
TSU09-OSL 1	HUB-0675	53,241713	13,97191	73	60	90 - 200	18.51 ± 1.13	21.15 ± 1.25	468.16 ± 10.32	0.19 ± 0.02	8.5 ± 4	2.16 ± 0.13	0.27 ± 0.02	20,9	0.26 ± 0.03	0.13 ± 0.01	0.12 ± 0.02
TSU09-OSL 2	HUB-0676	53,241713	13,97191	73	125	90 - 200	19.55 ± 1.37	21.74 ± 1.17	488.99 ± 11.08	0.18 ± 0.02	20.2 ± 5	2.04 ± 0.14	0.67 ± 0.03	17,9	-	0.33 ± 0.03	-
TSU17-OSL 1	HUB-0677	53,241387	13,97067	75	50	90 - 200	19.55 ± 1.62	22.19 ± 1.81	477.55 ± 11.21	0.19 ± 0.02	5.3 ± 4	2.22 ± 0.16	0.42 ± 0.02	5,0	-	0.19 ± 0.02	-
TSU17-OSL 2	HUB-0678	53,241387	13,97067	75	205	90 - 200	17.19 ± 1.65	19.24 ± 1.44	473.88 ± 10.46	0.17 ± 0.02	14 ± 5	2.01 ± 0.15	1.62 ± 0.03	8,5	-	0.81 ± 0.06	-

Protocol: Single Aliquot Regenerativ (SAR) according to MURRAY, A. S. & WINTLE, A. G., 2000. Luminescence dating of quartz using an improved single-aliquot regenerative-dose protocol. Radiation Measurements 32, 57 – 73.

Material: Quarz (90-200 µm), 'Coarse grain method'

Measurement device: Risø-TL/OSL-DA-15C/D, Dose rate of Sr-90-beta source: 0.089 Gy/s

Measurement parameters: Preheat 200°C/10s, Preheat test dose (cutheat): 160°C/0s, Stimulation: Blue diodes with emission maximum at 470nm, detection: near UV at 330nm

(*) after elimination of outliers (potential outlier > mean + 4*SD or < mean - 4*SD)

(**) sigma b = 0.2

Sample ID	Sample depth	Geogr. Position		Lab ID	14C age	Calibrated age (cal BP 2σ)	remarks	Material
	[cm]	Latitude	Longitude					
CHRI_647 130	130	53,356911	13,657911	Poz-67573	270 ± 30 BP	436 - 152 cal BP (95.4%)		charcoal
CHRI_647 163-164	163	53,356911	13,657911	Poz-67574	2920 ± 35 BP	3167 - 2960 cal BP (95.4%)		bulk peat
CHRI_647 185-187	186	53,356911	13,657911	Poz-67575	5950 ± 40 BP	6883 - 6676 cal BP (95.4%)		bulk soil
Raakow1 HK5	112	53,35666516	13,61792287	Poz-80793	410 ± 30 BP	520 - 429 cal BP (82.8 %) 373 - 368 cal BP (0.5%) 360 - 330 cal BP (12.1%)	0.14mgC	charcoal
Raakow2 HK1	98	53,35451506	13,63261217	Poz-80794	3455 ± 30 BP	3828 - 3640 cal BP (95.4%)		charcoal
Fkhg2 wood 1	180	53,35436237	13,75499769	Poz-80795	1150 ± 30 BP	1174 - 979 cal BP (95.4%)		wood
RKS-14C-1	350	53,308302	13,665362	Poz-80909	2910 ± 53 BP	3210 - 2920 cal BP (92.9%) 2909 - 2885 cal BP (2.5%)		plant remains
RKS-14C-3	288	53,308302	13,665362	Poz-80910	2575 ± 30 BP	2760 - 2698 cal BP (82.7%) 2633 - 2616 cal BP (4.1%) 2588 - 2538 cal BP (7.8%) 2527 - 2518 cal BP (0.9%)		Sphagnum moss
RKS-14C-4	251	53,308302	13,665362	Poz-80911	1580 ± 30 BP	1540 - 1404 cal BP (95.4%)		bulk peat
RKS-14C-5	196	53,308302	13,665362	Poz-80912	103.02 ± 0.36 pMC	254 - 225 cal BP (33.7%) 137 - 114 cal BP (25.2%) 106 - 99 cal BP (3.6%) 74 - 57 cal BP (19.9%) 44 - 32 cal BP (13%)	modern carbon	pine needles
RKS-14C-6	113	53,308302	13,665362	Poz-80913	1305 ± 30 BP	1293 - 1222 cal BP (66%) 1214 - 1181 cal BP (29.4%)		plant remains
NAU13 HK1	170	53,308144	13,664629	Poz-80914	775 ± 30 BP	736 - 669 cal BP (95.4%)	buried kiln	charcoal
Grauh1 HK8	150	53,39318082	13,5445372	Poz-80915	175 ± 30 BP	294 - 253 cal BP (18%) 225 - 136 cal BP (51.2%) 115 - 73 cal BP (6%) 34 cal BP - ...(20.1%)	too young	charcoal

Object_ID	Age category	Amount of dates	Study site	Latitude	Longitude	Reference
1	OSL	1	Klopzow	53,363889	12,762333	Küster 2014
2	OSL	10	Burgwall Kratzeburg	53,446861	12,958528	Küster 2014, Küster at al. 2015
3	OSL	8	Krummer See bei Kratzeburg	53,428389	12,970306	Küster 2014
4	OSL	11	Langhagen	53,388111	12,987417	Küster 2014
5	OSL	2	Großer Fürstenseer See	53,307444	13,158444	Kaiser et al. 2014
6	OSL	24	Serrahn	53,346722	13,18975	Küster 2014
7	OSL	5	Müritz - Schulzensee	53,310344	13,302656	Küster 2014
8	OSL	6	Waldsee	53,310139	13,304056	Küster 2014
9	OSL	24	Quillow catchment	53,356665	13,617923	this study
10	IRSL	5	Neuenhagener Oderinsel	52,850908	14,057633	Brose et al. 2002; Schatz 2000
11	IRSL	1	Wolfsschlucht	52,582031	14,089856	Schatz 2000
12	IRSL	31	Kleiner Tornowsee	52,580472	14,094539	Dreibrodt et al. 2010b
13	IRSL	14	Dahmsdorf	52,528361	14,102981	Schatz 2000
14	IRSL	15	Glasow	53,373219	14,252064	Bork et al. 1998
15	IRSL	8	Weltenburg	48,896931	11,821349	Lang 2003
16	IRSL	6	Vaihingen	48,933232	8,962298	Lang 2003
17	IRSL	11	Bauerbach	49,074144	8,742824	Lang 2003
18	IRSL	4	Bruchsal	49,106422	8,593351	Lang 2003
19	IRSL	5	Neurott	49,398609	8,587345	Lang 2003
20	IRSL	4	Walldorf	49,306369	8,642769	Lang 2003
21	IRSL	5	Wetterau	50,379449	8,912044	Lang 2003
22	IRSL	9	Amöneburg	50,797725	8,921994	Lang 2003
23	IRSL	5	Wiesenbach	49,361423	8,802814	Lang 2003
24	OSL	27	Baar	48,002699	8,463783	Henkner et al. 2017
25	OSL	17	Butzbach	50,41728	8,660652	Kühn et al. 2017